THE Journal OF THE AMERICAN LEATHER CHEMISTS ASSOCIATION

December 2022 Vol. CXVII, No.12 *JALCA* 117(12), 505–548, 2022

117th Annual Convention

to be held at the
Grand Geneva
Resort & Spa
Lake Geneva, WI
June 20–23, 2023

For more information go to:
leatherchemists.org/
annual_convention.asp

Contents

Distributed by
University of CINCINNATI
LIBRARY PUBLISHING SERVICES

An imprint of the University of Cincinnati Press

ISSN: 0002-9726

Communications for Journal Publication

Manuscripts, Technical Notes and Trade News Releases should contact:
Mr. Steven D. Lange, Journal Editor, 1314 50th Street, Suite 103, Lubbock, TX 79412, USA
E-mail: jalcaeditor@gmail.com Mobile phone: (814) 414-5689

Contributors should consult the Journal Publication Policy at:
http://www.leatherchemists.org/journal_publication_policy.asp

Beamhouse efficiency takes perfect balance.

Making leather on time, on spec and within budget requires a careful balance of chemistry and process. Buckman enables tanneries to master that balance with our comprehensive Beamhouse & Tanyard Systems. They include advanced chemistries that not only protect the hide but also maximize the effectiveness of each process, level out the differences in raw materials and reduce variations in batch processing. The result is cleaner, flatter pelts. More uniform characteristics. And improved area yield.

In addition, we offer unsurpassed expertise and technical support to help solve processing problems and reduce environmental impact with chemistries that penetrate faster, save processing time, improve effluent and enhance safety.

With Buckman Beamhouse & Tanyard Systems, tanneries can get more consistent quality and more consistent savings. Maintain the perfect balance. Connect with a Buckman representative or visit us at **Buckman.com**.

1945 2020 Buckman75

JOURNAL OF THE
AMERICAN LEATHER CHEMISTS ASSOCIATION

Proceedings, Reports, Notices, and News
of the
AMERICAN LEATHER CHEMISTS ASSOCIATION

THE JOURNAL OF THE AMERICAN LEATHER CHEMISTS ASSOCIATION (USPS #019-334) is published monthly by The American Leather Chemists Association, 1314 50th Street, Suite 103, Lubbock, Texas 79412. Telephone (806)744-1798 Fax (806)744-1785. Single copy price: $8.50 members, $17.00 non-member. Subscriptions: $185 for hard copy plus postage and handling of $60 for domestic subscribers and $70 for foreign subscribers; $185 for ezine only; and $205 for hard copy and ezine plus postage and handling of $60 for domestic subscribers and $70 for foreign subscribers.

Periodical Postage paid at Lubbock, Texas and additional mailing offices. Postmaster send change of addresses to The American Leather Chemists Association, 1314 50th Street, Suite 103, Lubbock, Texas 79412.

Website: www.leatherchemists.org E-mail: carol.adcock@ttu.edu

COLD
Milling

Smooth Leather Milling

Erretre
Tannery Innovations

Erretre s.p.a. | Via Ferraretta,1 | Arzignano (VI) 36071 | tel. +39 0444 478312 | info@erretre.com

Effects of Calcium Content on the Enzymatic Bating of Delimed Hides

by
Chunxiao Zhang,[1,2,3]* Buqing Ye,[1,2] Jinzhi Song[1,2] and Biyu Peng[1,2,3]*
[1]*National Engineering Laboratory for Clean Technology of Leather Manufacture, Sichuan University*, Chengdu 610065, P. R. China
[2]*Key Laboratory of Leather Chemistry and Engineering of Ministry of Education, Sichuan University*, Chengdu, Sichuan 610065, P. R. China
[3]*College of Biomass Science and Engineering, Sichuan University*, Chengdu, China

Abstract

The effects of calcium content on the enzymatic bating of delimed hide were analyzed by amino acid analysis, tissue staining, and scanning electron microscopy–elemental energy spectrometry. Results show that the content and form of calcium in pelt can affect enzyme activity. The content of calcium in pelt can be adjusted by phosphoric-phosphate deliming to reduce the degree of damage caused by enzymes to elastin and collagen. The calcium bound in pelt can be further removed by deliming using a calcium chelator, thus effectively improving the efficiency of enzyme action. When the calcium content is lower than 0.6%, the removal degree of elastin by enzymes and the loosening effect to collagen fiber can be significantly improved. This research offers important guidance to improve the leather bating process.

Introduction

Tanning is the process of processing the collagen matrix of animal skin into leather products of practical value. To obtain high-quality leather products, the hair, epidermis, fibrous stroma, grease, and other non-collagen components in the skins have to be removed through processes such as soaking, degreasing, unhairing and liming, deliming, bating, and pickling, while collagen fiber could be opened up moderately according to the requirements for finished leather.[1] Then, the pelts are prepared for tanning and promoting the infiltration and bonding of leather chemicals in collagen matrix to improve the properties of crust leather.

Bating is the process of deliming pelts through enzyme preparations (mainly trypsin), and it is the only biotechnology that, as of now, cannot be replaced by chemical treatment.[2] The essence of its biochemical reaction is that, with the use of proteases, non-collagen components such as elastin, keratin, glycoprotein, albumin, and globulin in skins and hides are further destroyed or removed, the collagen is hydrolyzed and the collagen fibers are further opened up to the desired degree,[3,4] determining the overall style and basic sensory properties of the finished leather. Therefore, bating is one of the essential operations in the conventional leather manufacturing process and one of the most difficult processes to control in leathermaking.

In general, the bating operation is conducted under pH conditions of 7.0–9.0 at 30°–40°C.[5] However, the properties of leathers, including softness, fullness, and tightness, always vary with raw hides and the varieties and styles of finished leather. The enzyme dosage, bating temperature, pH, and time are usually adjusted to fulfill the requirements of different leather properties according to the tanners' experience. For example, upper leathers and other leathers with a high degree of tightness can easily soften, while leathers with higher softness requirements, such as sofas and clothing, needs a longer time to satisfy basic requirements, easily causing damage to the grain.[6,7]

At present, trypsin with high specificity to peptide bonds is mainly selected for use in the bating process of leather.[8] For a long time, the main goal has been to find a new protease to replace trypsin. Therefore, the research emphasis of bating technology is the screening of biological enzymes and the exploration of the optimal operating conditions in the bating process.[9-10] However, the influence of the substrate characteristics (the state of delimed pelt) on the enzymatic bating has not received sufficient attention. Studies have shown that the calcium ion (Ca^{2+}) can combine with the carboxyl group of collagen side chain under alkaline conditions, which changes the surface charge of collagen fiber. It can improve the resistance to enzymatic hydrolysis of collagen fiber and effectively protect the grain surface during enzymatic unhairing.[11] Through a simulation of the biomineralization mechanism, a porous and insoluble calcium phosphate protective layer can form on the surface of collagen fiber, which can also improve the enzyme resistance of collagen fiber.[12] In the unhairing-liming process, to loosen collagen fibers effectively, adding a large amount of lime is often necessary for the treatment of alkali expansion, resulting in a large calcium content of limed pelt.[13] In the deliming process, the calcium in the limed skin will be partially dissolved and removed under the action of acid-base neutralization, dehydration deswelling, and so on. However, its removal degree will be greatly different because of the type of delimed agent and degree of deliming, thus affecting the effect of enzymatic bating.

Therefore, in this research, the degree of calcium removal within the delimed pelt was purposefully controlled, and the effect of calcium removal degree during deliming on the effect of enzymatic bating

*Corresponding Author e-mail: chunxiaozhang@scu.edu.cn, pengbiyu@scu.edu.cn
Manuscript submitted May 12, 2022, accepted for publication June 14, 2022.

was investigated by various means, such as protein (desmosine and hydroxyproline) analysis, histological staining, and scanning electron microscopy–energy dispersive X-ray spectroscopy (SEM-EDS) analysis. This research provides a scientific basis for improving the controllability of the bating process for different styles of leather.

Materials and Methods

Materials

Salted-wet cattle hides from Sichuan, China, were purchased from a local tannery (Chengdu Xinshi Leather Industry CO., Ltd.), and were carefully chosen from reliming stage and the rest of the beamhouse operations were carried as per commercial leather making procedure reported previously.[15] Ethylenediaminetetraacetic acid disodium solution (EDTA-Na, 10 g/L, pH=8.0-8.5), Elastase (210,000 U/g, pH8.0, 40°C, Novozymes Co.), Trypsin (360,000 U/g, pH8.0, 40°C, Novozymes Co.), the chrome tannage, syntans, fatliquors, polymers and filling agents used in this experiment were industrial grade while the rest of the chemicals were analytical grade.

Methods

Preparation of delimed pelt with different calcium contents

Four pieces of relimed cow hides were taken from symmetrically adjacent parts along the back line, marked and weighed, and washed twice with 200% (the weight of limed hide) water at 30°C for 30 min each time. Then, the water dosage was controlled to 50% of the mass of limed hides, and the deliming process was performed at 33°C in four thermal cycle stainless steel quadrupole drums (GSD, Wuxi Xinda Light Industry Machinery Co., LTD., China). The methods are as follows:

(1) The appropriate amounts of sodium dihydrogen phosphate and 10% phosphoric acid solution were added in the drum and rotated for 240 min to infiltrate evenly. The pH was controlled to about 8.0–8.5 (the same below), and then the samples were washed with 200% water 3 times, 30 min each time.

(2) The 2.5% ammonium sulfate was added in the drum, which was rotated for 40 min, and then drained. The samples were washed with 200% water for 30 min, redelimed with 1.5% ammonium sulfate under the same conditions, and washed with water 3 times. Other operating conditions are the same as (1).

(3) The 2.5% ammonium sulfate was added in the drum, which was rotated for 40 min, and then drained. The samples were washed with 200% water for 30 min. The redeliming was performed combined with 1.0% ammonium sulfate and 1.0% EDTA-Na under the same conditions and then washed 3 times.

(4) The samples were pre-delimed with 2.5% ammonium sulfate and 1.0% EDTA-Na to be rotated for 40 min and drained. The samples were washed with 200% water for 30 min. The redeliming was performed combined with 0.5% ammonium sulfate and 2.0% EDTA-Na under the same conditions and then washed 3 times.

Effect of calcium content of pelt on bating

The delimed pelts were dropped into four drums. The liquid ratio was 50%, and the temperature was 35°C. The activity concentration of trypsin and elastase was controlled to 20 U/mL, and the samples were rotated for 240 min. The pH of the bath solution was measured every 60 min, and 5.0 mL bath solution was extracted as reserve. Then, the samples were drained and washed with 200% water twice, 30 min each time. The hides were extracted as reserve. Subsequent processes, such as acid dipping, chrome tanning, retanning, fatliquoring, and drying, were performed according to the process of creating bovine sofa leather.[14]

Evaluation of deliming effect

(1) Evaluation of deliming degree of different methods

Ten points were marked on the pelt, and the thickness of each point was measured before and after deliming. Then, the degree of deliming was characterized by the average of thickness change rate of the 10 points.

$$\text{Change rate of thickness (\%)} = \frac{\text{the thickness of washed redelimed pelt} - \text{the thickness of washed delimed pelt}}{\text{the thickness of washed redelimed pelt}} \times 100$$

(2) Quantitative analysis of calcium content and distribution in delimed pelt

After being freeze-dried at −55°C and 20 Pa, the skin was evenly divided into three layers by a precision splitting machine (C520L, Camog (a) Inc., Italy). After cutting and ensuring a constant weight of each layer, the sample was accurately weighed and fully digested with sufficient nitric acid and hydrochloric acid at 120°C to form a clear solution. Then, the volume was fixed to 100 mL after cooling. The calcium concentration of the digested solution was measured by the AES-ICP method, and the calcium content of each layer in pelt was further calculated.[15,16]

(3) EDS analysis of calcium in delimed pelt[17]

After being freeze-dried, the delimed pelt was cut into samples of appropriate size. After being sprayed with copper, plane scanning of calcium element was performed by using an SEM-EDS energy spectrometer (Scanning Electron Microscope and X-ray Energy Dispersive Spectroscopy, JSM-7500F/X-MAX50, JEOL, Japan) with a control time of 5 min.

Evaluation of bating process

(1) Determination of soluble protein content in bating bath

The bating bath was centrifuged at 3500 rpm for 5 min every 60 min, and the supernatant was diluted with an appropriate amount. The soluble protein content of the bath was determined by Folin-phenol assay.[18]

(2) Determination of hydroxyproline and desmosine in bating bath

A total of 1.50 mL of bating bath was centrifuged at 8000 rpm for 6 min, and 1.0 mL of concentrated hydrochloric acid (12 mol/L) was added to 1.00 mL supernatant. The bath was fully dissolved at 120°C for 12 h. After deacidification, concentration, and dilution, the concentrations of hydroxyproline and desmosine in the bath were measured by using an A3000 amino acid analyzer (MembraPure, Germany).[19]

(3) Staining analysis of bated pelt tissue sections

The bated pelt was fixed with 10% neutral formaldehyde at room temperature for 24 hours, and the sections were cut into approximately 12 μm thick pieces in the longitudinal direction by using freezing microtome (CM1950, Leica, Germany). After drying, the skin was dyed by using the hematoxylin-eosin method and alkaline fuchsin method. Then, the distribution of elastic fibers and the dispersion degree of collagen fibers were observed by using an optical microscope.

(4) EDS analysis of carbon elements in bated pelt

The bated pelt was freeze-dried and cut into samples with an appropriate size. After being sprayed with copper, surface scanning of carbon elements on the cut surface was performed by using an SEM-EDS energy spectrometer with a control time of 5 min.

(5) Evaluation of grain pattern of the crust leather

The samples of the dried crust leathers of each tanning group were viewed microscopically using Desktop Phenom Pro Desktop Scanning Electron Microscope (Phenom Pro, Phenom World Inc., Netherland) to evaluate the grain pattern on the surface of leather samples.

Results

Property analysis of the delimed pelt

Bating is a heterogeneous catalytic reaction process in which the enzyme penetrates into the delimed pelt and acts on the corresponding substrate. The thickness, pH, and temperature of the delimed pelt have a great influence on the enzymatic activity. As can be seen from Table I, the four deliming methods, which use phosphoric acid-sodium dihydrogen phosphate, ammonium sulfate, and different amounts of EDTA-Na, can effectively neutralize the alkali in the limed hides. The pH of pelt can be controlled at 8.2–8.4, and the phenolphthalein was colorless in the vertical incision of pelt. After washing, the average thickness of the delimed hide was between 1.2 mm to 1.3 mm, and the thickness change rate of each delimed hide was between 31% to 37%. The four deliming methods achieved comparable deliming degrees on the limed hides, and the overall state of each delimed pelt is relatively similar, thus laying the foundation for further study on the influence of calcium content of pelt on enzyme action.

After being freeze-dried, the delimed pelt was evenly divided into three layers by using a precision layer splitting machine, and the calcium content of each layer was measured. The results shown in Figure 1 indicate that the calcium content of pelt is about 1.1% after deliming with sodium dihydrogen phosphate (method I). After two times of deliming with ammonium sulfate (method II), the calcium content of pelt was reduced to about 0.6%. When 1.0%

Table I

Deliming effectiveness of the series of methods

Deliming method*	I	II	III	IV
Deliming pH	8.2	8.3	8.4	8.4
Thickness of delimed hide (mm)	1.3	1.2	1.2	1.3
Thickness change rate of pelt (%)	33	35	37	31

*Deliming method: I - phosphate - sodium dihydrogen phosphate deliming, II - 2.5% ammonium sulfate pre-deliming, 1.5% sulfuric acid compound deliming, III - 2.5% ammonium sulfate deliming, 1.0% ammonium sulfate combined with 1.0% neutral EDTA-Na complex deliming, IV – 2.5% ammonium sulfate combined with 1.0% neutral EDTA-Na pre-deliming, 0.5% ammonium sulfate combined with 2.0% neutral EDTA-Na complex deliming,

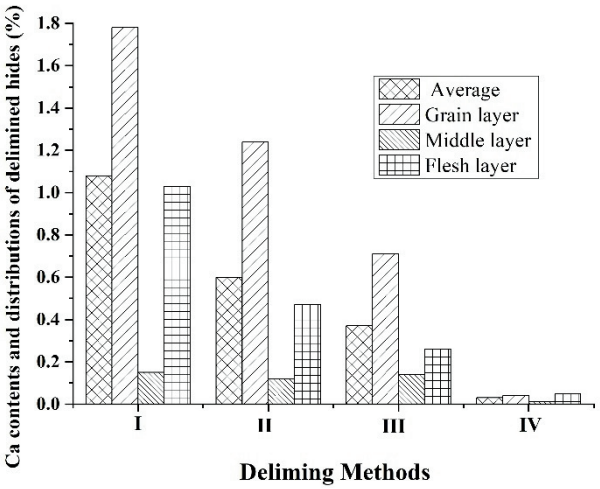

Figure 1. Ca content and distribution of delimed hide

EDTA-Na (method III) was used in redeliming with ammonium sulfate, the calcium content of pelt was further reduced to about 0.4%. When the neutral EDTA was sufficiently used in both pre-deliming and redeliming, which used ammonium sulfate (method IV), the calcium in pelt is almost completely removed, and the residual calcium content is about 0.03%. However, the calcium content in the middle layer of each delimed pelt was similar (except for method IV), and the difference of calcium content was mainly reflected in the difference of calcium content on the surface of the pelt.

The calcium ions were analyzed by using X-ray EDS (Figure 2). As the degree of calcium removal intensified, the calcium signal density at the incision was significantly reduced. When sodium dihydrogen phosphate was used in the deliming process, the distribution signal density of calcium in the papillary layer was significantly stronger than that in the middle and flesh sides, which shows that, deliming with sodium dihydrogen phosphate leads to calcium precipitation in the papillary layer. When ammonium sulfate was used alone for deliming (II), the signal density of calcium was stronger, and the signal density of calcium on both sides was relatively larger. This result occurred mainly because the calcium content on both sides of limed skin is higher than that of the middle layer, which was not effectively removed by deliming with ammonium sulfate alone. When combined with neutral EDTA-Na treatment of pelt (III and IV), the signal density of calcium in pelt was significantly reduced, and the uniformity was significantly increased, thereby again proving that EDTA could effectively remove calcium from the inside and the outside of pelt, while sodium dihydrogen phosphate mainly caused calcium precipitation on the surface of pelt. Therefore, the calcium content of pelt can be linearly changed by different deliming methods, and the bating effect of protease on delimed skin with different calcium content can be further investigated.

Effect of calcium content of pelt on enzymatic bating

After deliming, the main component of pelt is fibrous collagen, followed by elastin, which is mainly distributed in the papillary layer, and the interstitial proteins that have not been sufficiently removed. During the bating process, under the action of enzymes, non-structural proteins such as glycoprotein, albumin, and globulin within the pelt will be destroyed, and the structural proteins such as elastin and collagen will be partially dissolved, resulting in increased concentration of soluble proteins or peptides in the bath. Therefore, the combination of high-purity trypsin and microbial protease with high elastin activity was selected to bate the delimed pelt with different calcium contents. The overall effect of the enzymatic bating on the pelt could be analyzed by measuring the soluble protein content in the bath. As can be seen from Figure 3, with the decrease in the calcium content of pelt, the concentration of soluble protein in the bath increases sequentially, showing that the high calcium

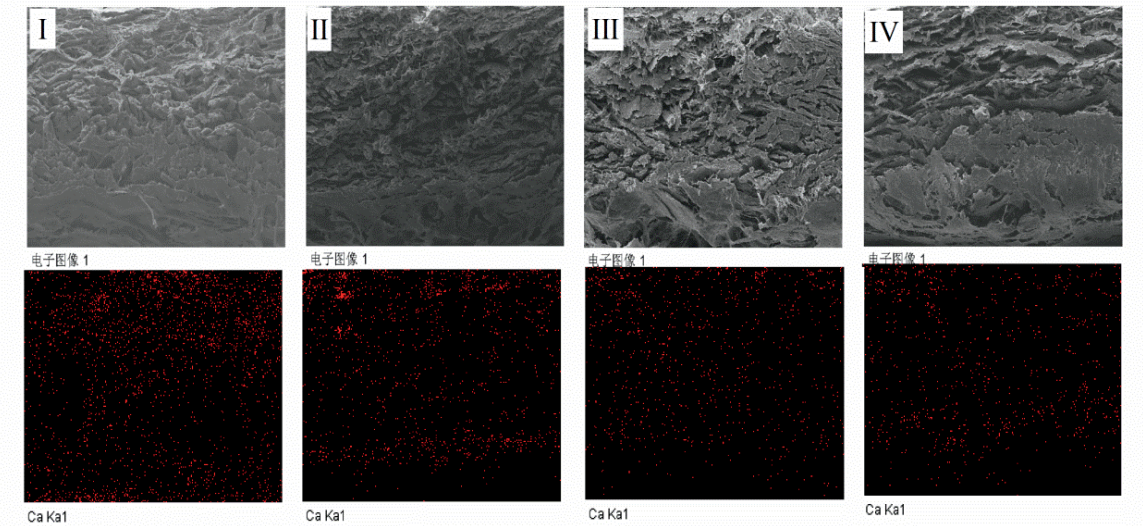

Figure 2. SEM-EDS analysis of the calcium on the bated pelts' longitudinal section

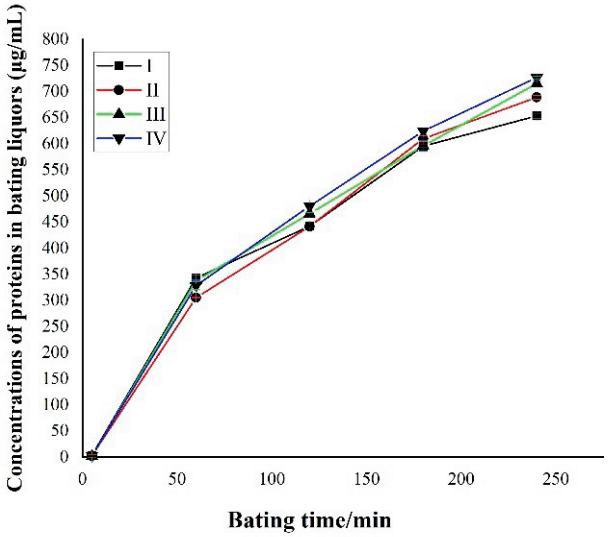

Figure 3. Concentrations of soluble protein in bating baths

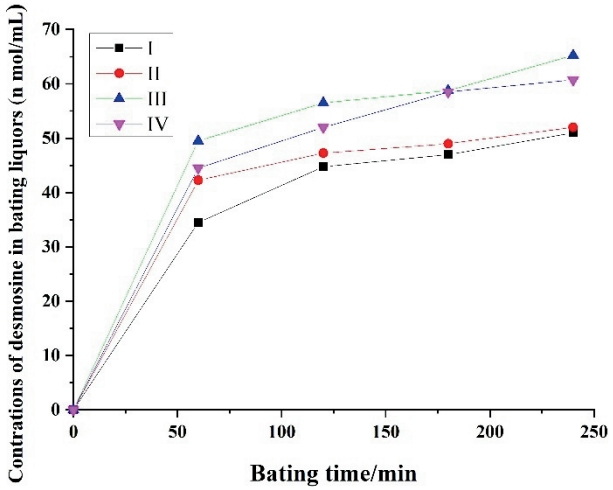

Figure 4. Effects of Ca content in grain layer on concentrations of desmosine in bating baths

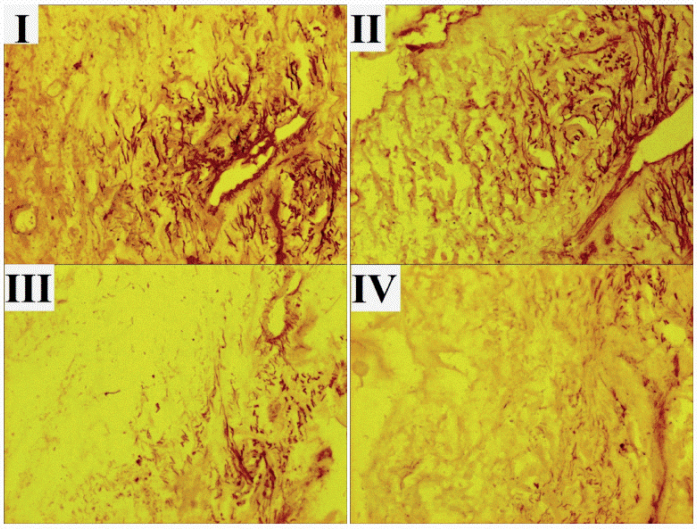

Figure 5. Elastin analyze of the bated pelt section (20 × 10)

content of delimed pelt will affect the enzymatic effect on the protein components of skin. However, when the average calcium content within delimed pelt was above 0.6%, the concentration of soluble protein in bath was relatively slow. When the calcium content of pelt was below 0.6%, the concentration of soluble protein increased rapidly.

Influence of calcium content of pelt on enzymatic bating with elastase

Elastin is a structural protein component in delimed pelt, second in abundance after collagen and is mainly distributed in the papillary layer. Its content has a great impact on the elasticity, compactness, and shaping of leather. Elastin has good acid and alkali resistance and can generally only be hydrolyzed by enzymes during the leathermaking process. Elastin contains desmosine. Thus, the hydrolysis rate of elastin by enzymes can be determined by analyzing the desmosine content in the bating bath. As can be seen from Figure 4, the concentration of desmosine in hydrolysate increased with the enhancement of the calcium removal from the grain layer. However, when the calcium content of the grain layer was above 1.2%, the calcium content of the pelt on the grain layer had no obvious influence on the action of enzyme on elastin. When the calcium content in the grain layer (Figure 1) decreased from 1.8% to 1.2%, the content of desmosine increased from 51 n mol/mL to 52 μg/mL only. When the calcium content decreased to 0.7%, the concentration of desmosine increased sharply to about 65 n mol/mL, indicating that strengthening the removal of calcium in pelt during deliming can significantly enhance the effect of protease on elastin.

The changes in the elastin fibers, which were derived by the bating of pelt with different calcium contents, were further reflected by histological staining results (Figure 5). As the degree of deliming increased, the elastic fibers of the bated pelt were destroyed to a greater extent. After deliming with sodium dihydrogen phosphate (I) and ammonium sulfate (II), the structure of elastic fibers of bated pelt remained relatively intact. The elastic fibers of bated pelt were almost completely destroyed when the calcium content within pelt was low after the deliming process combined with EDTA. This result was consistent with the trend in the concentration of hydrolysate (desmosine) in the bating bath.

Effect of calcium content of pelt on the collagenase effect

The main component of delimed pelt is collagen, which is also the main object of processing and utilization in leather production. The degree of hydrolysis directly affects the overall quality and style of leather, and is the main control point in the bating process, which is adjusted according to the performance requirements of different leather species. Therefore, the hydrolyzation of collagen were evaluated by hydroxyproline concentrations in the liquors and Histological staining, the results are shown in Figure 6 and Figure 7.

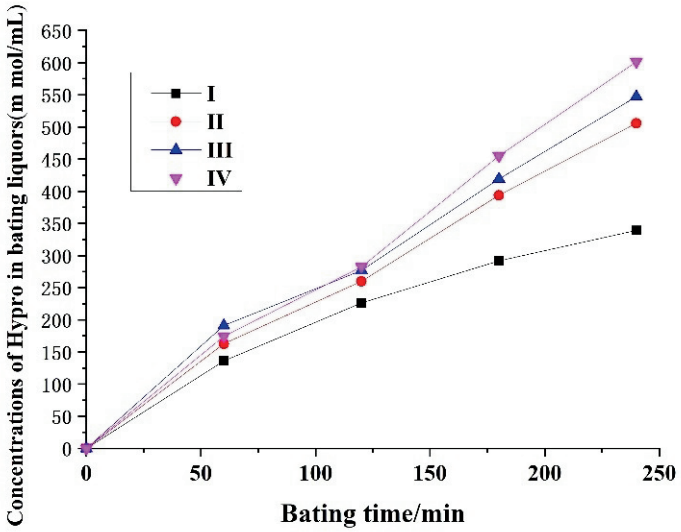

Figure 6. Effects of Ca content in delimed pelts on concentrations of hydroxyproline in bating baths

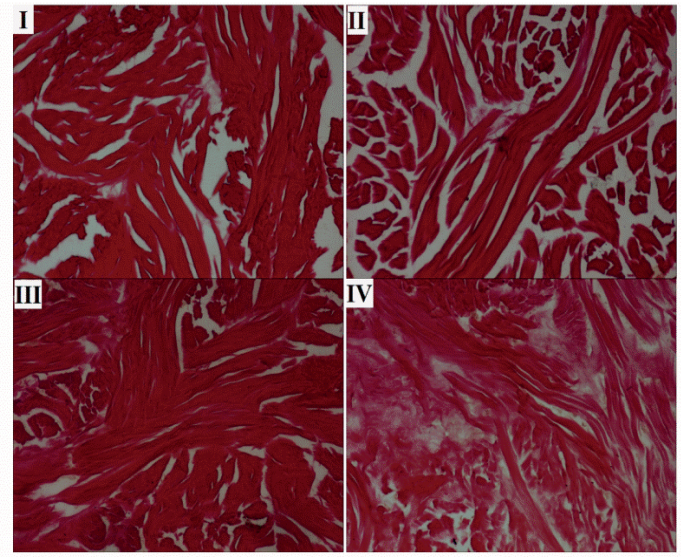

Figure 7. Collagen analysis of the bated pelts section (20 × 10)

As can be seen from Figure 6, the hydroxyproline in the bating bath increased gradually with the decrease in the calcium content of delimed pelt. Histological staining (Figure 7) showed that after enzymatic treatment, the fibrous bundles of bated pelt were thicker and showed a complete "bundle bar" when the calcium content of pelt was greater (I and II). However, with the decrease in the calcium content, the loosening of the collagen fibrous bundles gradually increased. When the calcium content was reduced to about 0.4% (III), the bunch-bar shape of the fibers started to be destroyed, and the fiber bundle showed a better loosening effect. When the calcium was completely removed from the delimed pelt (IV), the collagen fiber bundles dispersed into loose filaments. The carbon (C) elements in bated pelt were further analyzed by SEM-EDS, and the results (Figure 8) showed that when the calcium content was above 0.6% (I and II), the carbon signal density of the incision after the bating process was greater, and the difference was not obvious. This finding indicates that the dispersion degree of the fibers in the pelt had minimal difference. The carbon signal density on the incision of bated pelt decreased significantly with the further decrease in the calcium content, indicating that the fiber dispersion was enhanced.

As mentioned before, excessive hydrolysis on collagen by enzymes result in damaging grain is one of the potential risks of bating. The electron micrographs (Figure 9) illustrate that with the decrease of calcium content in the delimed pelts, the leather grains are damaged, the patterns are not smooth and clearly visible. Therefore, the grain patterns would be protected from

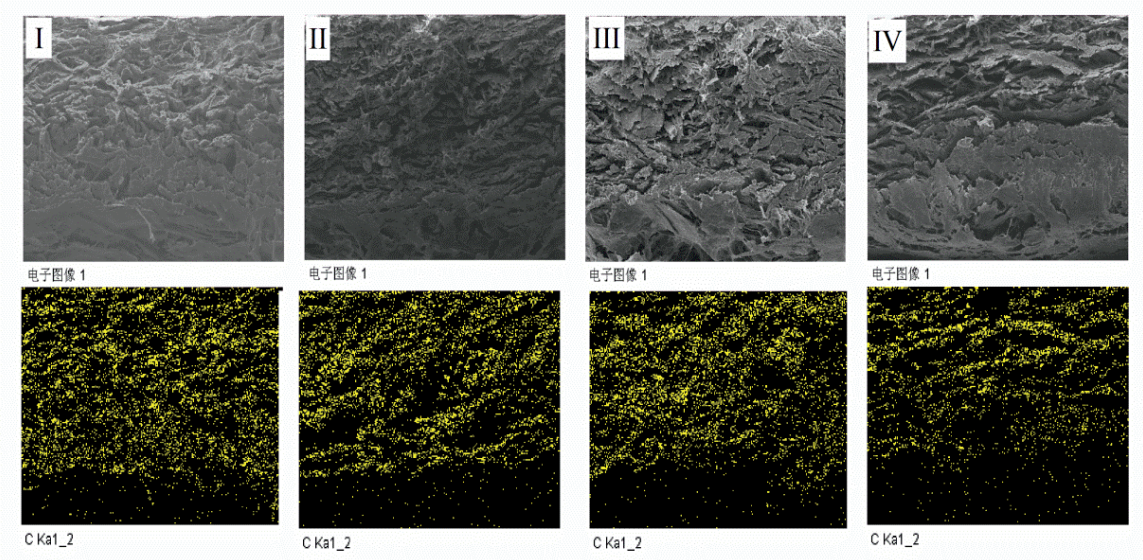

Figure 8. SEM-EDS analysis of carbon on the bated pelts' longitudinal section

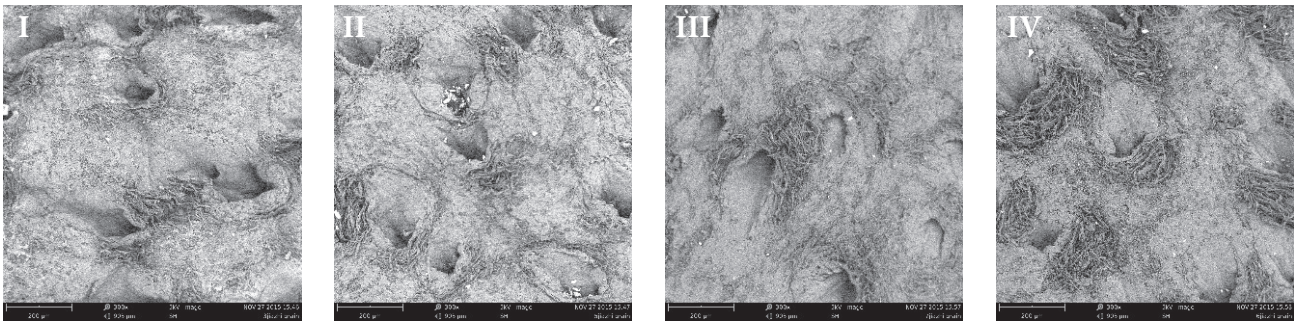

Figure 9. SEM images of grain pattern of crust leather (×300, 5KV)

being damaged by the deposited Ca with phosphate, which would be removed during pickling.[11]

Analysis of enzymatic mechanism of delimed pelt by calcium content and its practical application

Bating is one of the most difficult processes to control in the leather preparation process. The enzymatic degree on collagen and elastin needs to be adjusted in time according to the performance requirements of different leather species, and improving the controllability and safety of the bating process are always the main concern in leather production.

In the limed pelts, calcium exists in three forms, including free calcium ions, dissolved/adsorbed calcium hydroxide, and calcium bound to collagen. The calcium bound to collagen changes the surface charge of collagen fibers, and weak cross-linkages formed between collagen fibers. Thus, the enzyme resistance of collagen fibrils improved.[21] In the conventional deliming process using ammonium sulfate, the free calcium ions and calcium hydroxide in the limed skin can be effectively removed by neutralizing and dehydrating, but the calcium ions bound to collagen cannot be effectively removed. In the deliming process with phosphoric acid and phosphate, calcium phosphate precipitates are formed in the pelt (especially on the surface of the pelt) to coat the protein surface, which hinders the enzymatic effect to a certain extent (Figure 3). However, this method does not make the calcium bound to structural proteins, such as collagen and elastin within the pelt, rather it makes the enzymatic effect non-significant. In the deliming combined with ammonium sulfate and EDTA-Na (methods III and IV), the calcium bound to proteins within the pelt could be removed more effectively through the chelation of calcium by EDTA-Na.[22] This approach reduces the enzyme resistance of collagen and elastin, and significantly enhances the enzymatic effect.

For the production of leather items with high grain tightness requirements, such as shoe upper leather, it is necessary to improve the binding efficiency of calcium ion with the pelt, enhancing the enzyme resistance of collagen and elastin, which prevents the excessive enzymatic effect on elastin and collagen during the bating process. In the preparation of leather products such as garment leather, sofa leather, and leather where grain spreading and leather softness are required, a calcium chelating agent should be used to enhance the degree of calcium removal and improve the enzymatic efficiency.

Controlling the calcium content of delimed pelt can effectively regulate the effect of enzymes on elastic fibers and collagen fibers. This study is of great significance to ensure uniform enzymatic action during the bating process.

Conclusion

The calcium content of delimed pelt can be controlled effectively by using phosphoric-phosphate, ammonium sulfate, and EDTA-Na during the deliming process. The calcium content of delimed pelt can affect the performance of enzymes during the bating process. Adjusting the content and form of calcium in delimed pelt enables the regulation of the degree of enzymes' action on collagen and elastin during the bating process, thus improving the controllability of the bating process of different leather species.

Acknowledgements

This work was financially supported by National Natural Science Foundation of China (21908149), China Postdoctoral Science Foundation (2018M633366, 2018T110974) and National Key R&D Program of China (2017YFB0308402). The authors acknowledge Jinwei Zhang for his support of the mechanical operation during leather manufacturing.

References

1. Luo, F.X., Zhong, X., Gao, M.C., Peng, B.Y., Long, Z.Z.; Progress and mechanism of breaking glycoconjugates by glycosidases in skin for promoting unhairing and fiber opening-up in leather manufacture. A review. *J Leather Sci Eng*, **2**:12, 2020.
2. Song, Y., Wu, S., Yang, Q. et al.; Factors affecting mass transfer of protease in pelt during enzymatic bating process. *J Leather Sci Eng*, **1**:4, 2019.
3. Wilson, J. A. The mechanism of bating. *JALCA*, **12**: 1087-1090, 1920.
4. Sizeland K H, Edmonds R L, Basil-Jones M M, Kirby N, et al.; Changes to collagen structure during leather processing. *J Agric. Food Chem*. **63**, 2499–505, 2015.
5. Li, F.Y., Shi, L.W., Tao, H.D., Xu, K.H., Lei, X.Y.; Reducing the risk of grain damage during bating of Leather Manufacturing: an alternative to pancreatic enzymes with alkaline protease from novel *Bacillus Subtilis SCK6*. *JALCA* **115**(9): 315-323, 2020.
6. Wilson J A, Merrill H B.; Another important role played by enzymes in bating. *Journal of Industrial and Engineering Chemistry*, **18**: 185-188, 1926.
7. Dettmer A, Ayub MAZ, Gutterres M.; Hide unhairing and characterization of commercial enzymes used in leather manufacture. Braz J Chem Eng. **28**:373–80, 2011.
8. Renicke C, Spadaccini R, Taxis C.; A tobacco etch virus protease with increased substrate tolerance at the P1' position. *PLoS One*.8:e67915, 2013.
9. Kamini N R, Hemachander C, Geraldine Sandana Mala J, Puvanakrishnan R.; Microbial enzyme technology as an alternative to conventional chemicals in leather industry. *Current Science* **77**, 80-86, 1999.
10. Jaouadi N Z, Rekik H, Elhoul M B, Rahem F Z, et al.; A novel keratinase from Bacillus tequilensis strain Q7 with promising potential for the leather bating process. *Int. J Biol. Macromol.* **79**, 952–64, 2015.
11. Gao, M.C., Tian, Y.X., Zhang, X., Zhang, C.X, Peng, B.Y.; A substrate protection approach to applying the calcium ion for improving the proteolysis resistance of the collagen. *Applied Microbiology and Biotechnology*, **105**, 9191–9209, 2021.
12. Nudelman, F., Lausch, A.J., Sommerdijk, N.A.J.M., et al.; In vitro models of collagen biomineralization. *Journal of Structural Biology*, **183**(2): 258-269. 2013.
13. Tian, Y.X., Gao, M.C., Zhang, X., Peng, B.Y., Zhang, C.X., Chen, Y.K.; Effect of Calcium Salt Mineralization on protease resistance of hide collagen fibers and enzymatic unhairing. *LEATHER SCIENCE AND ENGINEERING,* **31**(3):1- 6, 2021.
14. Zhang, C.X., Lin, J., Jia, X.J., Peng, B.Y.; A Salt-free and chromium discharge minimizing tanning technology: the novel cleaner integrated chrome tanning process. *J. Clean. Prod.* **112**. 1055-1063, 2016.
15. Zhang, C.X., Xia, F.M., Peng, B.Y., Shi, Q., Cheung, D., Ye, Y.B.; Minimization of chromium discharge in leather processing by using methane sulfonic acid: a cleaner pickling-masking-chrome tanning system. *JALCA*, **111**: 435-446, 2016.
16. Zhang, C.X., Xia, F.M., Long, J.J., Peng, B.Y.; An integrated technology to minimize the pollution of chromium in wet-end process of leather manufacture. *J. Clean. Prod.* **154**: 276-283, 2017.
17. Zhang, C.X., Hu, J.M., Yu, D.S., Xia, C., Sadaquat, A.C., Peng, B.Y.; Exploration of the diffusion, binding and crosslinking of chromium complex within hides during chrome tanning. *JALCA* **114**(5): 180-188, 2019.
18. Li, Y.H., Zhang, C.X., Luo, F.X., Peng, B.Y.; A new approach for quantitative characterization of hydrolytic action of protease to elastin in leather manufacture. *Appl Microbiol Biot*, **102**(24): 10485-10494, 2018.
19. Li, Y.H, Jia, X.J., Peng, B.Y.; Covalent immobilization of organophosphorus hydrolase onto insoluble bovine collagen fibers. *JALCA* **109**: 197-206, 2014.
20. Witold, D., Zenon, G., Barbara, B.; Degradation of TN-C component of troponin by trypsin. *Biochimica Et Biophysica Acta*, **490**: 216-224, 1977.
21. Yan, W., Joe M. R.; Effect of EDTA, HCL, and citric acid on Ca salt removal from Asian (silver) carp scales prior to gelatin extraction. *The Society for Food Science and Technology*, **74**: C426-C431, 2009.

Feasibility Assessment of the Identification of the Source of Condensed Tannins in Leathers by FTIR Spectroscopy and Chemometrics

by
Alireza Koochzakzaei,[1,*] Mohammadamin Sabbaghiyan Bidgoli[1] and Siyamak Safapour[2]
[1]*Faculty of Cultural Materials Conservation, Tabriz Islamic Art University*, Tabriz, I.R. Iran.
[2]*Faculty of Carpet, Tabriz Islamic Art University*, Tabriz, I.R. Iran.

Abstract

This study aimed to investigate the feasibility of identifying the type of plant used in the tanning of leathers by cost-effective Fourier transform infrared (FTIR) spectroscopy. The investigation was performed on European horse-chestnut (fruit peel), mimosa, and quebracho and three specimens of mimosa-tanned leathers. Tannin extraction from plants was performed in an ultrasonic bath using acetone-water solvent (70%). Tannin extraction from leathers was carried out from the corium fibers using acetone-water solvent (1:1). After extraction, filtration, centrifugation, and solvent removal, the samples were subjected to FTIR spectroscopy. Principal Component Analysis (PCA) and hierarchical clustering were used to identify the source of tannins based on FTIR results. In addition to FTIR spectra, their first and second derivatives were also used in statistical analyses. The obtained FTIR spectra and their derivatives and the results of PCA and hierarchical clustering showed that rich plant sources of condensed tannins can be well differentiated by spectroscopy in the fingerprint region (700-1800cm^{-1}). The PC1-PC2 plot in the analysis of FTIR spectra and the PC2-PC3 plot in the analysis of derivatives showed the best ability to differentiate and identify the extracts. Multivariate PCA and cluster analyses performed well in identifying the type of plant used in the tanning of the studied leathers, especially when applied to the derivatives of FTIR spectra.

Introduction

Tannins are polyphenolic compounds produced in plants as secondary metabolites.[1] The synthesis and accumulation of these compounds are influenced by a variety of factors including photosynthesis, season, temperature, and rainfall.[2] Tannins can be extracted from various parts of almost all plants including roots, stems, leaves, and secretions. Tannins are generally classified into two groups: hydrolysable and condensed. Hydrolysable tannins themselves can be divided into two sub-groups: gallotannins and ellagitannins. Hydrolysable tannins are extracted from plants like chestnut, sumac, tara, and myrobalan. Sources of condensed tannins include mimosa, quebracho, hemlock, alder, willow tree, and gambir.[3,4] Condensed tannins, which classify as naturally occurring proanthocyanidins, are polyflavonoids composed of a chain of flavan-3-ol units. The most common proanthocyanidins are those composed of catechin or epicatechin chains interlinked by C4 → C6 or C4 → C8 bonds.[5] These tannins are typically joined by C4 → C8 bonds, but this may also occur through C4 → C6 bonds.[6]

Because of their relatively high molecular weight (between 500 and 3,000 Daltons),[7] tannins can form strong complexes with carbohydrates and proteins.[8] The oldest application of plant tannins was in the tanning of rawhide to stabilize animal skin proteins against decay.[3] Plant tannins have generally been the most commonly used group of tanning agents in leather processing before the nineteenth century.[4,9] However, the choice of the type of plant used in the tanning process could be influenced by a variety of factors including climate, predominant vegetation, culture, availability, economic condition, target quality, and target application.

Therefore, one issue of concern in the study of leather products, especially historical leather artifacts, is how to identify the type of plant used in the tanning process; information that can provide valuable insights into the above-mentioned factors. Some efforts have been made in this regard and there are indeed several reports of successful use of chromatographic and mass spectrometric methods for this purpose.[10-13] However, in addition to being quite expensive, these methods require extensive preparation and have their own limitations. In addition, identifying the type of tannin, and not the source of the plant used in tanning, has been one of the topics of interest to researchers. In previous studies, spectroscopic methods including FTIR and UV-Vis have been used to identify the type of tannin present in the leather structure.[14-16] Using these methods, it is indeed possible to well identify the type of tannin and determine whether it is condensed or hydrolysable (gallotannin or ellagitannin). In addition to spectroscopic methods, there are also reports of the successful use of various spot tests including ferric, vanillin, butanol acid, rhodanine, and nitrous acid tests to identify the type of tannin used in leathers.[6,17,18]

However, the great majority of studies on leather artifacts that have used spot tests and spectroscopic methods have been mainly focused on identifying the type of tannin used in tanning rather than the type of source plant. Research on tannins obtained from

*Corresponding author emails: Alireza.k.1989@gmail.com; a.koochakzaei@tabriziau.ac.ir
Manuscript received April 17, 2022, accepted for publication June 25, 2022.

different plants has shown that spectroscopy-based chemometrics can be used to identify and classify extracts based on the type of source plant. These studies have generally used FTIR, UV-Vis, and NIR spectroscopy methods.[19-21] However, considering their good performance in classifying plant extracts, chemometric methods can also provide a good estimate of the source plant of tannins used in leathers through statistical analysis of spectroscopic data. In this study, the goal was to assess the feasibility of identifying the type of plant used in the tanning of a leather product through FTIR spectroscopy and chemometric methods. In the first phase of this feasibility study, the assessments are performed on tannins extracted from mimosa, quebracho, and European horse-chestnut and three specimens of mimosa tanned leather.

Materials and methods

Tannin extraction

Tannins used in the study were extracted from three plants, namely quebracho, mimosa, and European horse-chestnut (fruit peel). The three leather specimens used in the study were produced by tanning goat and sheep hides with mimosa tannins (tanned in 2016). The characteristics of the specimens are given in Table I.

For tannin extraction from plants, 10mL of acetone-water solution (70%) was added to 200mg of the powdered plant substance in a sealed container, which was then placed in an ultrasonic bath. The extraction process was performed using Makkar [22] method in two 10-minute intervals with a 5-minute rest. The extract was filtered by a Whatman filter paper grade 42, and the filtered extract was then centrifuged at 3000 rpm for 10 min. The centrifuged solution was separated and placed in an oven at 70°C for one hour for solvent removal.

Tannin extraction from leather was performed using water-acetone solution (1:1) and samples collected from collagen fibers of the reticular layer. For every 10 mg of leather fiber, 1 mL of the solution was added to the sample.[10,15] The extraction was performed in a sealed container at standard laboratory temperature over a period of 48 h, during which the samples were placed on a shaker. Afterward, solution filtering and centrifugation and solvent removal were performed in the same way as described in the previous paragraph for tannin extraction from plants.

FTIR spectroscopy and multivariate analysis

Fourier transform infrared spectroscopy was used to examine the molecular structure of the samples. For this purpose, tannins extracted were examined using the KBr pellet method. To make the plate, the extract and KBr powder were mixed in a ratio of 1:100 w/w. This analysis was performed using a Jasco 680-plus FTIR spectrometer (Jasco Inc., Japan). The spectra were recorded in 64 scans with a resolution of $2cm^{-1}$ in the range of $400\text{-}4000cm^{-1}$.

Spectrum analysis was performed using the software Omnic9 and Originpro2021. After baseline correction, smoothing, and normalization to the 0-1 range, spectra first and second derivatives were obtained. Normalization of spectra intensity was performed to reduce the effect of tannin content in KBr plates. The spectra as well as their first and second derivatives were analyzed by Principal Component Analysis (PCA) and hierarchical clustering. In PCA, three components were extracted and the discriminatory power of different components in two dimensions was assessed using covariance and correlation matrices. Spectral analysis was performed in the fingerprint region ($700\text{-}1800cm^{-1}$).

Table I

Characteristics of the studied plants and leathers

Sample type	Source	Origin	Code
Plant	Mimosa	Italy	MI-N
	Mimosa	Italy	MI-Y
	Mimosa	Italy	MI-H
	Quebracho	South Africa	KE-N-1
	Quebracho	South Africa	KE-N-2
	European horse-chestnut (fruit peel)	India	PB-HEND-1
	European horse-chestnut (fruit peel)	India	PB-HEND-2
Leather	Goat Leather	Tabriz, Iran	L-G 1
	Goat Leather	Tabriz, Iran	L-G 2
	Sheep Leather	Tabriz, Iran	L-Sh

Results and discussion

First, FTIR spectra were used to investigate the presence of condensed tannins in the specimens. The presence of tannin can be detected by the appearance of absorption peaks at 1606-1615 assigned to aromatic ring stretch vibrations, 1507-1518 due to skeletal vibration of the aromatic rings, 1196-1211 and 1030-1043cm^{-1} assigned to stretching vibrations of the C–O bond. In addition to these peaks, which are related to the general structure of tannins, condensed and hydrolysable tannins also have their own characteristic peaks. More specifically, the presence of two peaks at 1704-1731cm^{-1}, assigned to carbonyl stretching vibrations, and 1317-1325cm^{-1}, assigned to the symmetric stretching of the C–O bond of the ester function, indicates a hydrolysable tannin, which will be a gallotannin if additional peaks appear at 1082-1088, 870-872, and 758-763cm^{-1} and an ellagitannin otherwise. FTIR spectra of condensed tannins show, in addition to the characteristic peaks of tannins, three absorption peaks at 1283-1288, 1155-1160, and 1110-1116cm^{-1} and two other weak peaks at 976 and 842-844cm^{-1}. These bands can be assigned to the ethereal C–O asymmetric stretching vibration arising from the pyran-derived ring structure.[3,14,15] FTIR spectra of the studied specimens in the 700-1800cm^{-1} range after baseline correction are shown in Figure 1a. Given the presence of characteristic absorption peaks of condensed tannins in these spectra, condensed tannins can be considered the dominant compound in the specimens.

PCA and Cluster plots obtained from the FTIR spectra in the 700-1800cm^{-1} range are shown in Figure 2. The purpose of PCA conducted based on PC1 and PC2 is to identify plant extracts (tannins) that are chemically similar to each other, which makes it possible to differentiate and determine the types of source plants based on the

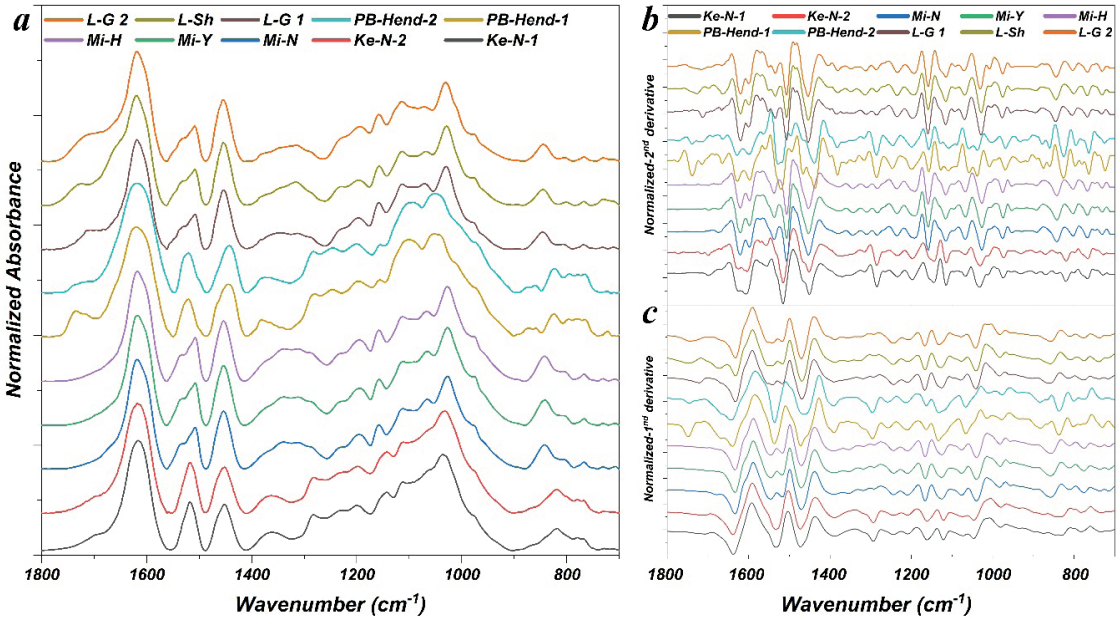

Figure 1. FTIR spectra of the condensed tannin extracts obtained from plants and leathers in the 700-1800cm^{-1} range after baseline correction **(a)**, the first derivative of the spectra **(b)**, the second derivative of the spectra **(c)**

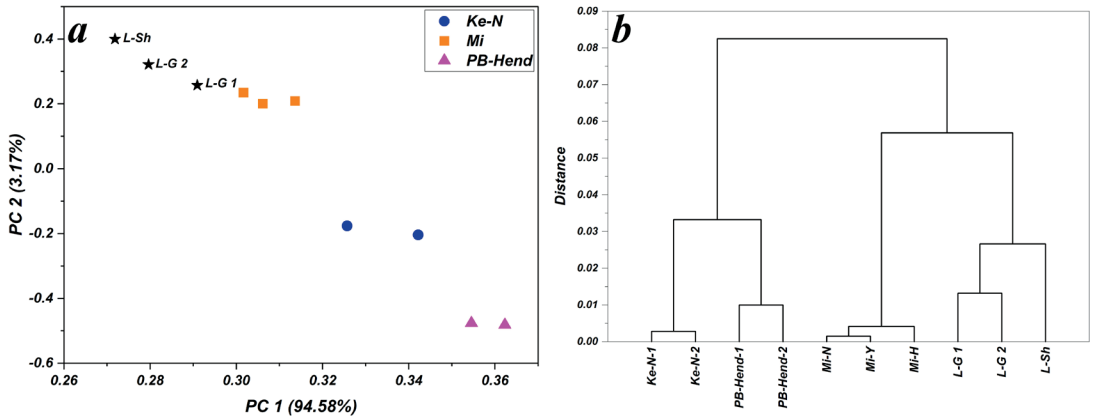

Figure 2. PCA plot **(a)** and hierarchical clustering plot **(b)** for the FTIR spectra of the condensed tannin extracts obtained from plants and leathers in the 700-1800cm^{-1} range

extracts. PCA results showed that tannins extracted from leathers have significant structural similarity to the one obtained from the mimosa plant. This is also well illustrated in the hierarchical clustering plot. These results indicate that among the studied plants, mimosa is most likely to be the source plant of the tanning agent used in the studied leathers.

The first and second derivatives of the spectra are displayed in Figures 1b and 1c. Using these derivatives, the differences and similarities of the spectra can be examined more closely with due consideration of overlapping peaks. Performing multivariate analyses on these derivatives results in more accurate differentiation and identification of compounds. PCA and Cluster plots obtained for the first and second derivatives of the spectra are shown in Figure 3. While for the spectra themselves PC1-PC2 provided good classification performance, for the first and second derivatives of the spectra, the best performance was observed in the PC2-PC3 plot. Compared to the PCA of the spectra, the PCA of the first derivative showed a higher correlation between tannins extracted from leathers and mimosa extract. This correlation was even higher in the PCA of the second derivative. This better performance of the derivatives, especially the second derivative, is also evident in hierarchical clustering results, where cluster plots show a decreasing gap between the extract obtained from leathers and mimosa tannins.

Therefore, considering the good performance of FTIR spectroscopy in identifying the type of tannin used in tanning, its source plant can also be determined by chemometric methods.

Conclusion

This study examined the feasibility of using FTIR spectroscopy-based chemometrics to identify condensed tannins used in the tanning of a leather product. Spectroscopy of the extracts obtained from three plant sources including mimosa, quebracho, and fruit peel of European horse-chestnut showed significant amounts of condensed tannins in these extracts. In addition to these plants, FTIR spectroscopy was performed on the extracts obtained from three specimens of roughly 6 years old mimosa tanned leathers, which were found to be rich in condensed tannins.

Principal component analysis and hierarchical clustering carried out using the obtained FTIR spectra showed that this could be a viable method to identify and classify plant species from which condensed tannins are produced. This differentiation and classification were performed through the analysis of fingerprint region spectra and their first and second derivatives. Interestingly, the multivariate analyses provided more accurate classifications when applied to the derivatives of the spectra, with the second derivative being the best

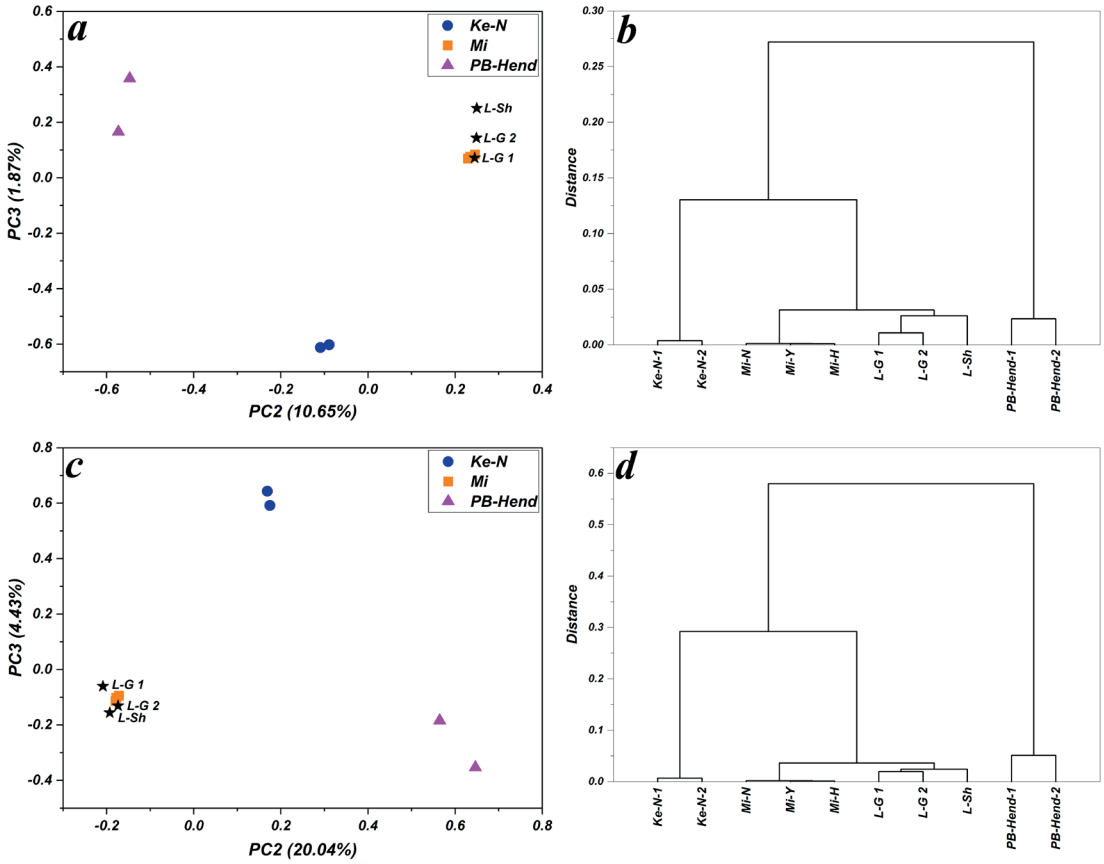

Figure 3. PCA and hierarchical clustering plots for the first derivative **(a, b)** and the second derivative **(c, d)** of the FTIR spectra of the condensed tannin extracts obtained from plants and leathers in the 700-1800cm^{-1} range

choice in this regard. The PC1-PC2 plot in the analysis of FTIR spectra and the PC2-PC3 plot in the analysis of derivatives showed the best ability to differentiate and identify the extracts. Therefore, in addition to being useful in the study of new leathers and identification of their plant sources, the combination of spectroscopic and chemometric methods can also be extended to identify the type of plants used in the tanning of historical leathers.

References

1. Hagerman, A.E. and Butler, L.G.; The specificity of proanthocyanidin-protein interactions. *J Biol Chem* **256**,4494-4497, 1981.
2. Mooney, H.A., Harrison, A.T. and Morrow, P.A.; Environmental limitations of photosynthesis on a California evergreen shrub. *Oecologia* **19**, 293-301, 1975.
3. Falcão, L. and Araújo, M.E.M.; Vegetable Tannins Used in the Manufacture of Historic Leathers. *Molecules* **23**, 2018.
4. Koochakzaei, A., Ahmadi, H. and Mallakpour S.; An Experimental Comparative Study of the Effect of Skin Type on the Stability of Vegetable Leather Under Acidic Condition. *JALCA* **113**, 345-351, 2018.
5. Garro Galvez, J.M., Riedl, B. and Conner, A.H.; Analytical Studies on Tara Tannins. *Holzforschung* **51**, 235-243, 1997
6. Falcão, L. and Araújo, M.E.M.; Tannins characterisation in new and historic vegetable tanned leathers fibres by spot tests. *J Cult Herit* **12**, 149-156, 2011.
7. Cano, A., Contreras, C., Chiralt, A. and González-Martínez, C.; Using tannins as active compounds to develop antioxidant and antimicrobial chitosan and cellulose based films. *Carbohydrate Polymer Technologies and Applications* **2**,100156, 2021.
8. Farooq, U., Shafi, A., Akram, K. and Hayat, Z.; Chapter 1 - Fruits and nutritional security, In: Fruit Crops: Diagnosis and Management of Nutrient Constraints, Srivastava AK, Hu C (Eds.). Elsevier Science, pp. 1-12, 2020.
9. Liénardy, A. and Van Damme, P.; Inter folia: manuel de conservation et de restauration du papier. Belgium: Institut royal du patrimoine artistique, 1989.
10. Wouters, J.; High-performance liquid chromatography of vegetable tannins extracted from new and old leathers. Proceedings of the 10th Triennal Meeting ICOM Committee for Conservation; 22–27 August Washington, DC, USA. London, UK: James & James for ICOM-CC. 1993.
11. Abdel-Maksoud, G.; Analytical techniques used for the evaluation of a 19th century quranic manuscript conditions. *Measurement* **44**, 1606-1617, 2011.
12. Sebestyén, Z., Badea, E., Carsote, C., Czégény, Z., Szabó, T., Babinszki, B., et al.; Characterization of historical leather bookbindings by various thermal methods (TG/MS, Py-GC/MS, and micro-DSC) and FTIR-ATR spectroscopy. *J Anal Appl Pyrolysis* **162**, 105428, 2022.
13. Sebestyén, Z., Jakab, E., Badea, E., Barta-Rajnai, E., Şendrea, C. and Czégény Z.; Thermal degradation study of vegetable tannins and vegetable tanned leathers. *J Anal Appl Pyrolysis* **138**, 178-187, 2019.
14. Falcão, L. and Araújo, M.E.M.; Application of ATR–FTIR spectroscopy to the analysis of tannins in historic leathers: The case study of the upholstery from the 19th century Portuguese Royal Train. *Vib Spectrosc* **74**, 98-103, 2014.
15. Falcão, L. and Araújo, M.E.M.; Tannins characterization in historic leathers by complementary analytical techniques ATR-FTIR, UV-Vis and chemical tests. *J Cult Herit* **14**, 499-508, 2013.
16. Melniciuc, N., Pui, A. and Florescu, M.S.; FTIR spectroscopy for the analysis of vegetable tanned ancient leather. *Eur J Sci Theol* **2**, 49-53, 2006.
17. van Driel-Murray, C.; Practical Evaluation of a Field Test for the Identification of Ancient Vegetable Tanned Leathers. *J Archaeol Sci* **29**, 17-21, 2002.
18. Koochakzaei, A. and Achachluei, M.M.; Red stains on archaeological leather: degradation characteristics of a shoe from the 11th–13th centuries (Seljuk period, Iran). *J Am Inst Conserv* **54**, 45-56, 2015.
19. Grasel, F.d.S., Ferrão, M.F. and Wolf, C.R.; Development of methodology for identification the nature of the polyphenolic extracts by FTIR associated with multivariate analysis. *Spectrochim Acta A Mol Biomol Spectrosc* **153**, 94-101, 2016.
20. Ricci, A., Parpinello, G.P., Olejar, K.J., Kilmartin, P.A. and Versari, A.; Attenuated Total Reflection Mid-Infrared (ATR-MIR) Spectroscopy and Chemometrics for the Identification and Classification of Commercial Tannins. *Appl Spectrosc* **69**, 1243-1250, 2015.
21. Grasel, F.d.S., Ferrão, M.F. and Wolf, C.R.; Ultraviolet spectroscopy and chemometrics for the identification of vegetable tannins. *Ind Crops Prod* **91**, 279-285, 2016.
22. Makkar, H.P.S.; Treatment of Plant Material, Extraction of Tannins, and an Overview of Tannin Assays Presented in the Manual. In: Quantification of Tannins in Tree and Shrub Foliage: A Laboratory Manual, Makkar HPS (Ed). Dordrecht: Springer Netherlands, pp. 43-48, 2003.

Simulation of Realistic Fur Texture Based on Piece Element Synthesis

by

Wei Wang[1,3], Weijie Wang[3], Gaopeng Zhang[3], Luming Yang[1,2,3]* and Biyu Peng[1,2,3]*

[1]*National Engineering Research Center of Clean Technology in Leather Industry, Sichuan University*, Chengdu 610065, China.

[2]*Key Laboratory of Leather Chemistry and Engineering of Ministry of Education, Sichuan University,* Chengdu 610065, China.

[3]*College of Biomass Science and Engineering, Sichuan University*, Chengdu 610065, China

Abstract

Realistic fur texture is usually modeled and rendered with three-dimensional software. Due to the complexity and inefficiency of the three-dimensional software, it cannot meet general designers' requirements to represent realistic fur texture quickly. In order to achieve the rapid drawing of real-quality fur, this work proposes an approach to simulating realistic fur texture based on the method of piece elements synthesis. To be specific, we used fur elements to represent fur units, the dislocation and superposition of which formed the fur visual effect. Also, we discuss the validity and feasibility of parameters that can be matched in Adobe Illustrator software. The method applied in this paper can not only meet the timeliness and convenience of designers when representing fur texture, but also visualize fur texture with a high sense of authenticity and diversity.

Introduction

Designers usually need to visualize realistic fur texture when representing product effects in a variety of fields, such as leather product design, fashion design, industrial design, graphic design, etc. Due to the character of fur with huge quantities, tiny radius, complex illumination, and mutual shadow, it is harder and slower to visualize fur texture than other kinds of surface textures.[1-5] At present, designers use either sketch, bristle brush or map rendering to demonstrate the complexity of fur.[3,6] However, designers need to pay great attention to drawing the geometric details of fur and to representing the invisible changes of light and shadow among fur, the heavy workload of which cannot meet designers' timeliness requirement when representing fur texture.

There exist several challenging problems for fur simulation in the field of computer graphics, including fur quantities, fur radius, fur density, complex illumination, and mutual shadow.[2,4,6,14] To represent realistic fur texture, researchers have done plenty of research on fur modeling and fur rendering.

Csuril represented each fur as a polygon patch in 1979.[7] After that, several researchers were trying to adopt different kinds of geometric elements to represent fur, such as pyramid,[8] curved cylinder,[9] trigonal prism,[10] etc. However, geometric details of fur were so complicated that it was difficult to achieve high processing speed based on computers, which resulted in dissatisfaction with real-time simulation. In 1997, Gelder proposed a geometric but simplified method to represent each fur as a polyline.[11] Although the technique met both real-time and interaction requirements, it lacked not only satisfactory results of fur authenticity but also a shortage of quantities. In addition to adopting geometric models, Reeves first introduced the particle system in 1983, which used simple but tiny particles as basic elements to represent irregular and fuzzy objects. The particle system originated from hydrodynamics, which had significant advantages in simulating fuzzy objects with highly efficient operation.[12] Since the system applied smoothly in real-time fur simulation, it has been widely used in fur modeling for many analysts and researchers. However, due to countless numbers of fur, using the particle system occupied plenty of computer memory.

In order to reduce the unnecessary costs of the particle system, some studies began to consider the use of texture to represent detailed characteristics of fur. In 1989, Perlin proposed that hyper texture could model phenomena intermediates between shape and texture by using space-filling applicative functions to modulate fur density.[13] He used pseudo-random function to control volume density of fur to generate fluffy objects. In the same year, Kajiya and Kay proposed a method for rendering scenes with sufficient fur detail via an item called Texel.[14] They represented one piece of fur as one Texel inspired by volume densities mixed with anisotropic lighting models to create realistic short-fur effect. However, the adoption of ray tracing rendering resulted in low velocity.

None of the above algorithms were provided with effective real-time performance. In order to achieve rapid simulation of fur, Meyer proposed a method of layered texture slicing based on Kajiya's foundation in 1998, which could represent objects with complicated micro-structures.[15] In terms of the idea of texture slicing, Lengyel proposed a layered shell approach that used multiple layers of texture to represent fur in 2000.[16] To be specific, he cut one piece of fur into several layers of two-dimensional texture and mapped those layers to different layers of mesh surfaces. At first, Lengyel applied particle systems to fur modeling. Then, he sampled fur modeling to generate shell texture. After that, he blended fur mesh surface

*Corresponding authors' email: pengbiyu@scu.edu.cn; ylmll1982@126.com

Manuscript received April 17, 2022, accepted for publication July 12, 2022.

and adopted an illumination model to simulate the lighting effect of fur, a real-time fluffy surface of an object could be generated. To improve the visual quality of the fur near silhouettes, Lengyel introduced lapped textures in 2001.[1] He used conventional two-dimensional texture maps to improve the appearance of silhouette seamlessly. The method produced fur images at an interactive rate for models of moderate complexity. Additionally, it allowed for real-time modification of viewing and lighting conditions, as well as local control of fur color, length, and direction.

Based on the inspiration of Lengyel's shell textures and lapped textures method, this paper proposes a simulation method for generating realistic fur texture based on the idea of piece element synthesis. Even though the concept originated from the research of Lengrel, it is different from Lengyel's method of simulating fur by layered piece fusion in a three-dimensional environment. That is, the authors adopted a method of displacing and superimposing fur elements in a two-dimensional environment to generate real-texture fur effect. The main contributions were as follows. Firstly, the geometric model of fur elements formed the fur visual effect by dislocation and superposition. Secondly, the volume element was converted into piece elements from three-dimensional simulation to two-dimensional simulation, which helped to reduce the number of calculations when processing real-quality fur. Thirdly, the relevant parameters of fur elements were set to control fur simulation results, so as to facilitate designers to simulate diversified fur texture with high efficiency.

As a new fur simulation method, firstly, a formation mechanism of real-quality fur was introduced based on optical principle. Secondly, in terms of the fur texture formation mechanism, the method of the dislocation and superposition of piece elements was applied to control the fur attributes by setting relevant parameters. Finally, the corresponding relationship between the theoretical parameters and the control parameters was analyzed in Adobe Illustrator software, which in turn verified the feasibility of the fur piece element synthesis method.

Method

Formation of the visual texture of fur

Due to the fact that human perception of the texture of an object comes from visual texture and tactile texture,[17] designers obtain the texture information of a perceived object mainly through their vision. Therefore, in order to accurately visualize the realistic texture of an object, it is of great necessity for designers to focus on the characteristics of an object's surface.

In the field of computer graphics, the simulation of an object's texture is one of the primary research contents for the area of photo-realism graphics. Based on Dana's research, an object's material properties and geometric structure determine its visual effect.[18] According to material properties, fur is constructed of fibers, as shown in Figure 1(a),[19] one single piece of fur has multiple-layer structure, which consists of Medulla in the center, Cortex in the

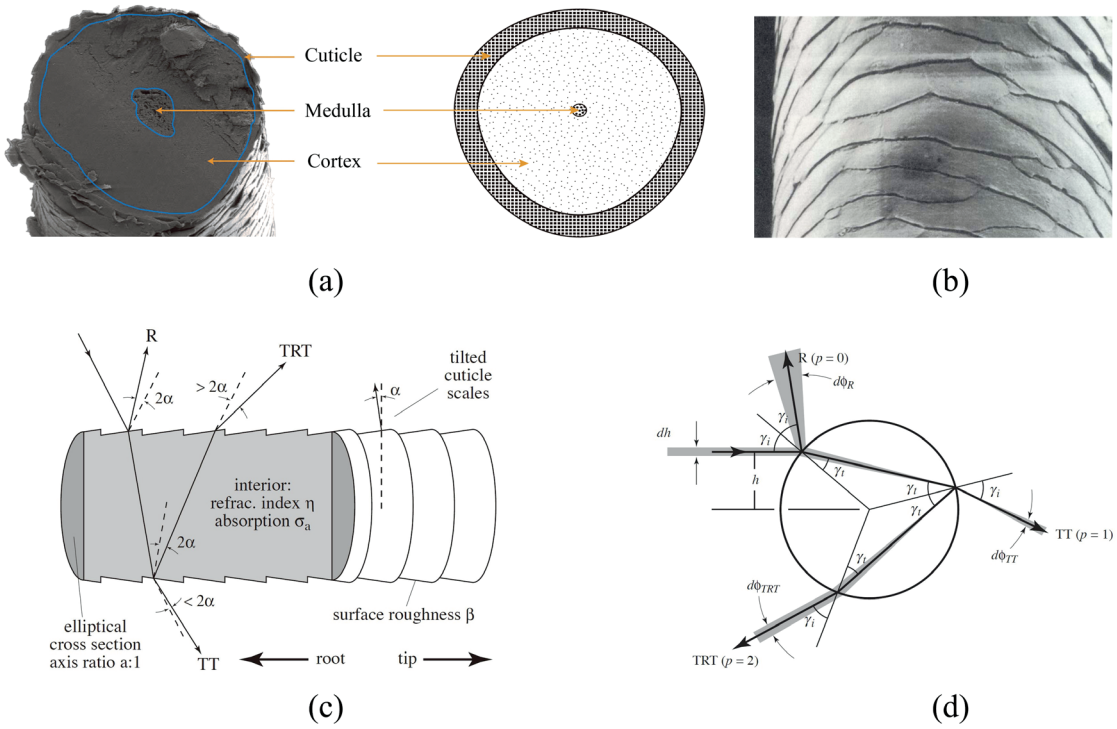

Figure 1. (a) Schematic diagram of a fur fiber cross-section **(b)** Cuticle scales of fur **(c)** Schematic diagram of simplified fur fiber model **(d)** Scattering diagram of light on the circular cross section of fur fiber

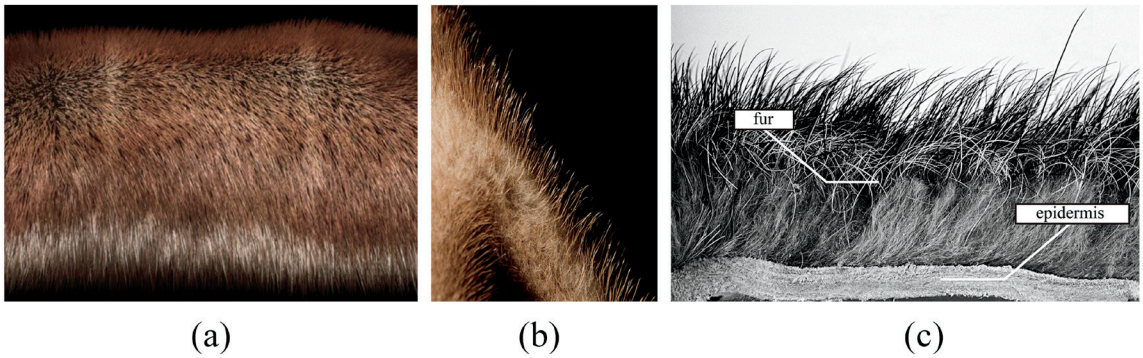

Figure 2. (a) Vertical view of brown mink fur **(b)** Close-up photos of brown mink fur **(c)** Cutaway picture of rawhide

interior, and Cuticle in the epidermis. To be specific, after the Cuticle is amplified, as shown in Figure 1(b),[19] pothole micro surfaces are visible, a medium that causes highlights and reflections. In addition, transmission and secondary reflection will occur after the light hits the surface of fur, as shown in Figure 1(c), (d).[20] We can generally think of fur as a scattering medium. That is to say, the light emitted vertically from the surface of fur will reach at the bottom part in an exponentially decreasing manner. In light of the vertical view of brown mink fur, as shown in Figure 2(a), (b),[21] lighter areas tend to be at the tip of fur, while darker areas tend to be at the root of fur. As a result, the characteristics of fur mentioned above together form its texture in human perceptions.

Research hypothesis

According to Jiang's research on the texture of objects, two factors that could affect the surface of an object are optical characteristics and geometric details.[22] In this study, we assume that the fur unit could be formed by plotting piece elements with geometric details and light features, and that fur texture could be formed by displacing and superposing fur unit at a certain distance. As shown in Figure 3, it shows the mechanism of fur vision formation.

Definition of fur texture model

As shown in Figure 2(c), fur and epidermis are the two geometric features of fur texture by analyzing a cutaway picture of rawhide. In order to simulate fur texture, we represented fur and epidermis with geometric figures. In this article, there are three levels defining and analyzing the fur element model.

Low-level parameter—circles and triangles

In terms of the fact that fur and epidermis are the two primary units of fur texture simulation, in order to simplify the method mentioned above, we used circles to represent epidermis and triangles to represent fur. As shown in Figure 4(a), (b), the attributes of circles and triangles include the coordinate of the center point P_i, the radius ξ_i, the coordinate of fur tip vertex T_i^j, and the coordinate of fur root vertex B_i^j and B_i^{j+1}.

Middle-level parameter—fur element

Since real fur grows on epidermis, we need to further define the fur element composed of fur and epidermis, as shown in Figure 4(b). Because the length and thickness of fur as well as the distance between fur pieces exist great differences, the texture of fur presents

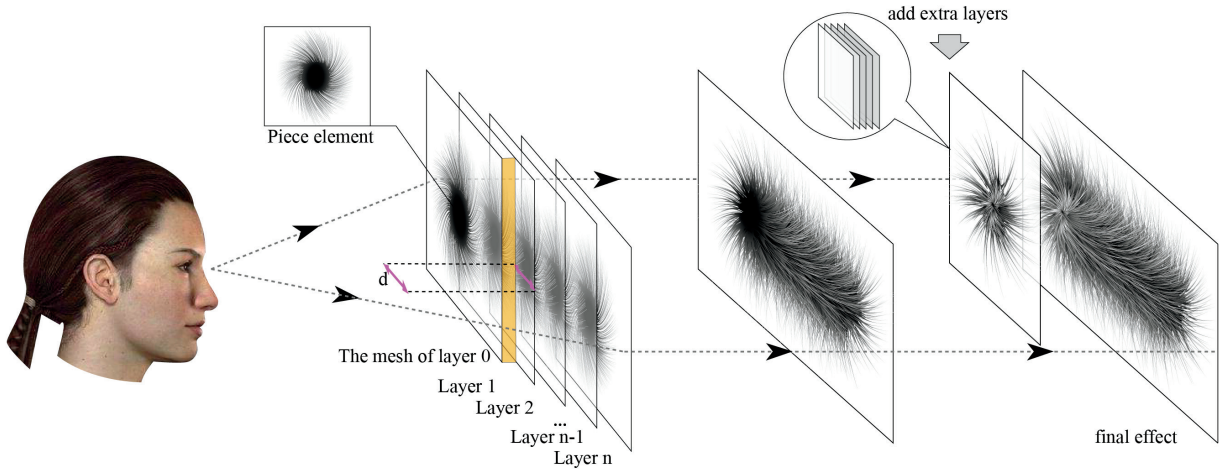

Figure 3. The mechanism of fur vision formation

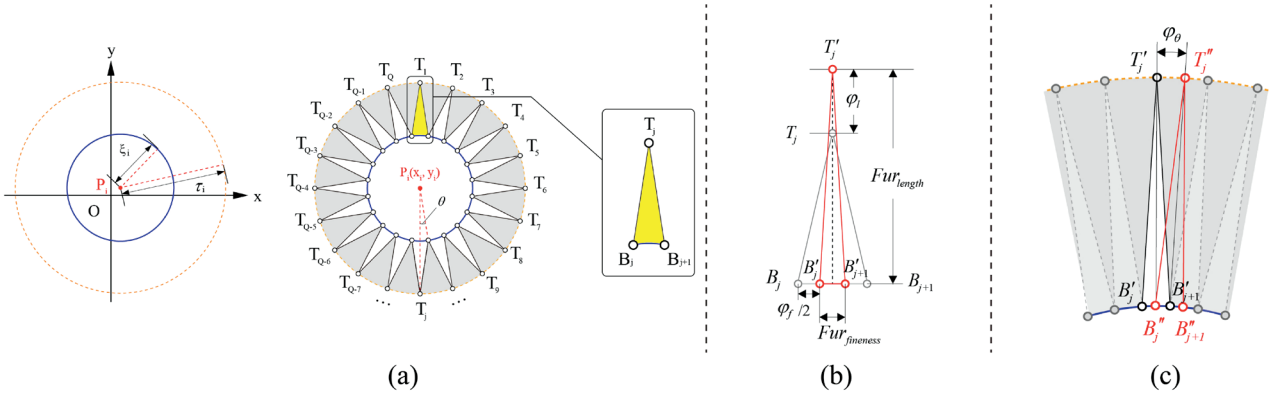

Figure 4. **(a)** The attributes of the base circle and the outer auxiliary concentric circle of fur piece elements **(b)** The angular attributes of fur piece elements **(c)** The principle of random variation of fur difference and related parameter settings

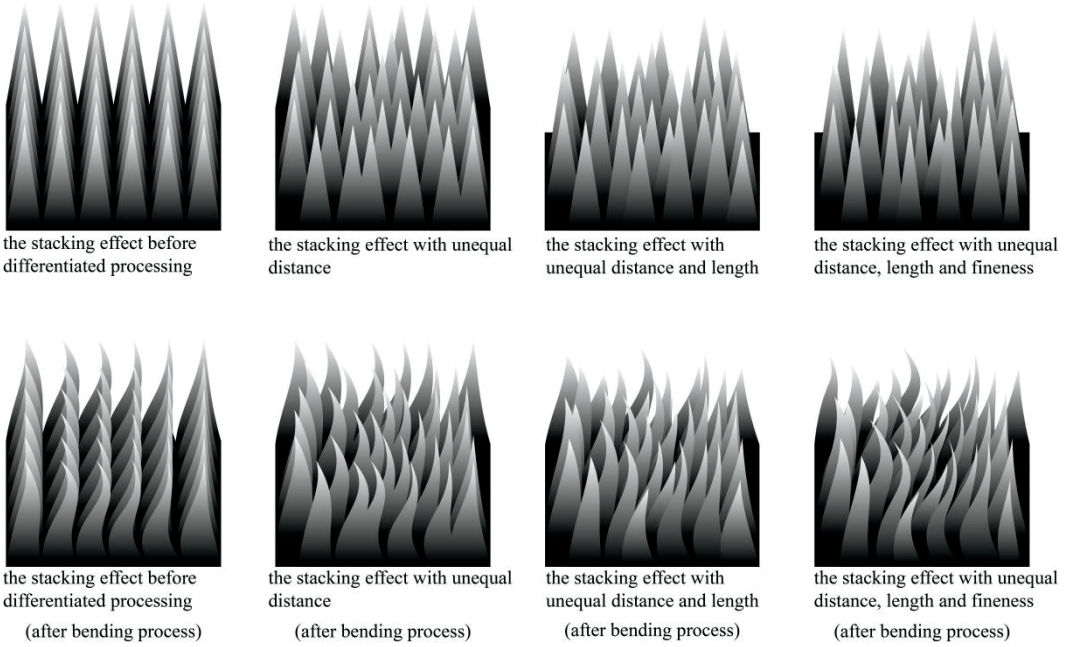

Figure 5. The establishment principle of fur difference

unevenly geometric characteristics. As shown in Figure 5, the effect of fur texture through differentiated processing presents strong irregularities. In this paper, in order to reflect the texture characteristics of real fur, it is necessary to control the difference between fur elements, which is also a significant factor of fur texture simulation. As shown in Figure 4(b), (c), the article defines the degree of difference between each fur piece from random changes in fur length, fur fineness, and fur displacement. The attributes of a composite fur element include the coordinate of the center point of the base circle P_i, the radius of the base circle ξ_i, the radius of the outer auxiliary concentric circle τ_i, the number of vertex of fur piece Num_{vertex}, the length of a single fur piece Fur_{length}, the fineness of a single fur piece $Fur_{fineness}$, the varying quantities of the length of a single fur piece φ_l, the varying quantities of the fineness of a single fur piece φ_f, the varying quantities of the rotation angle of a single fur piece φ_θ.

High-level parameter—fur element arrangement

The key step from the fur piece element to the formation of fur texture is to overlap the piece elements in a dislocation manner, so as to present the visual effect of fur texture. Therefore, based on the definition of one single fur element, it is of great necessity to define multiple high-level parameters to control the stacking arrangement of piece elements. According to the way of dislocation and superposition of fur elements, it can be divided into two categories including off-axis stacking and coaxial stacking, as shown in Figure 6(a). To be specific, off-axis stacking is that the radius of the base circle keeps constant, and the center of the base circle is overlapped by a certain internal distance, leading to an offset stack effect. In contrast, coaxial stacking is that the center of the base circle stays constant, and fur piece elements are gradually scaled and superposed by a certain proportion. As shown in Figure 6(b), each fur piece element has its own parameters, such as the center point

coordinate of the base circle, fur length, fur fineness, and fur density. Also, fur texture model includes several control parameters, such as the superimposition mode of fur piece element, the center point of the base circle, and the spacing among fur elements. At the same time, in order to control the roughness of fur, a control parameter that could randomly adjust the degree of fur difference is added to the fur texture model. In the process of constructing the fur texture model, we need to consider the simulation of optical characteristics of fur, in addition to the representation and definition of geometric details. As shown in Figure 6(c), the light gradually fades from the tip to the root of fur, so that fur has the lowest root brightness and the highest tip brightness. We can simulate the attenuation of light by filling fur piece elements with a black and white gradient from the center of the base circle to the outer auxiliary concentric circle. Due to the difference in the degree of light attenuation on fur under strong and weak light environments, the fur texture displayed quite discrepant. Therefore, it is necessary to set the light attenuation and degree parameters to control the light attenuation. As shown in Figure 6(d), $Dg_{\max}$ is the maximum value of the distance between the brightest pixel point and the auxiliary concentric circle edge in the strong light environment, and η is the luminance turning point. While $Dl_{\max}$ is the maximum value of the distance between the darkest pixel point and the center of the base circle in the weak light environment, and ϖ is the luminance turning point.

To sum up, key factors in fur texture model include the way of fur element dislocation and superposition, the coordinates of the center point of the base circle-fur element, the distance between fur elements, fur length, fur density, fur fineness, fur difference and light attenuation mitigation.

The texture model of fur is defined as $S = \{\ell, \zeta, \psi\}$, where $\ell = \{\omega, \vartheta, P_0, P_z, \xi, \delta, \rho, \chi, \gamma, \beta_+, \beta_-\}$, is the high-level set, the arrangement of fur piece elements which can be set through user interaction. To be specific, the parameter ω is the stacking mode of fur piece elements, which controls the dislocation and superposition mode of fur. The parameter ϑ is the distance between fur piece elements. When fur piece elements are offset stacking, it represents the distance between the center point of the base circle and the center point of the adjacent one. When piece elements are coaxial stacking, it means the length difference between the radius of the base circle of the adjoining sheet elements and the radius of the outer auxiliary circle. The parameter P_0 is the coordinate of the center point of the initial base circle. The parameter P_z is the coordinate of the center point of the initial base circle. The parameter ξ is the radius of the base circle, which controls the initial radius length of the base circle. The parameter δ is the length of fur, which controls the initial length of fur piece elements. The parameter ρ is the density of fur, which controls the initial density of fur. The parameter χ is the relative fineness of fur, a ratio type value, which controls the fineness of fur. The parameter γ is the fur diversity, which controls the random change on fur elements. The greater the difference is, the larger the roughness of fur texture is. The parameter β_+ is the attenuation mitigation of light on fur in the strong light environment, the larger β_+ is, the smaller $Dg_{\max}$ is, and the greater gradient transition is. The parameter β_- is the attenuation intensity of light on fur in the low light environment, the larger β_- is, the smaller $Dl_{\max}$ is, and the greater gradient intensity is.

$\zeta = \{FPE_i : i = 1, \cdots, Z\}$ is the set of middle-level parameters, known as the set of fur piece elements (FPE). The parameter set

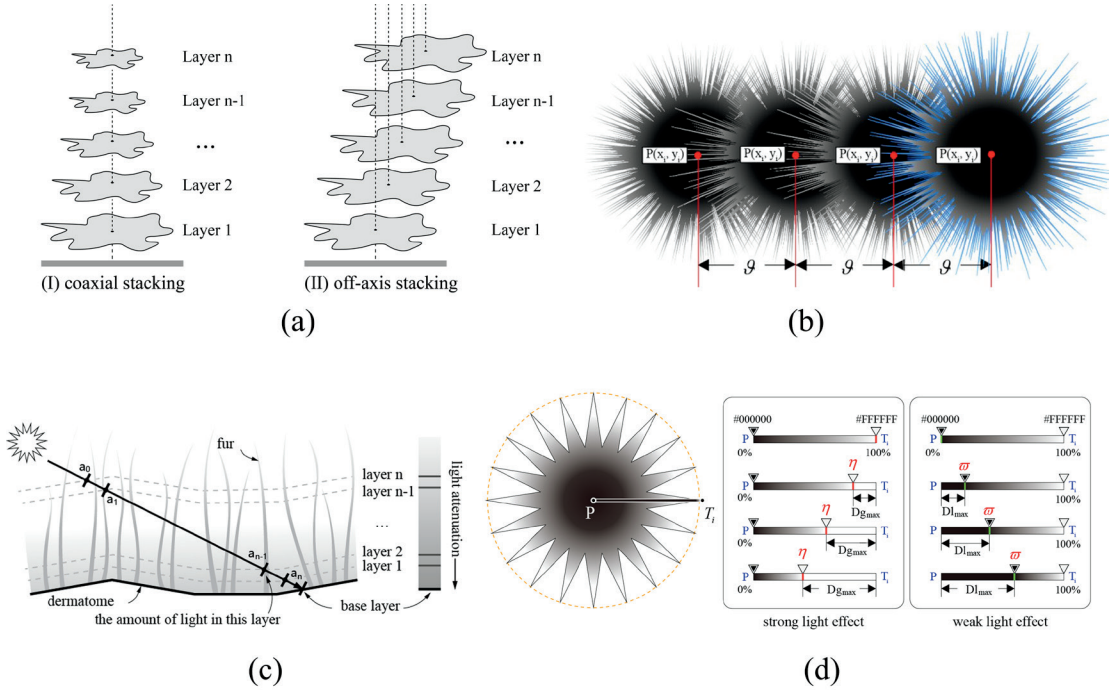

Figure 6. **(a)** Dislocation and superposition mode of fur piece elements **(b)** Schematic diagram of off-axis stacking spacing among piece elements **(c)** Schematic diagram of light attenuation from fur tip to fur root **(d)** Parameter declaration of light attenuation mitigation

for each fur piece element is $FPE_i = \{P_i, \xi_i, \tau_i, Num_{vertex}, Fur_{length}, Fur_{fineness}, \varphi_l, \varphi_f, \varphi_\theta\}$. To be specific, the parameter P_i is the coordinate of the center point of the base circle. The parameter ξ_i is the radius of the base circle, determined by the three parameters, including the superposition mode parameter ω, the spacing parameter ϑ, and the radius parameter ξ of the base circle in ℓ. The parameter τ_i is the outer auxiliary concentric circle radius, determined by the four parameters, including the radius parameter ξ, the superposition mode parameter ω in ℓ, the spacing parameter ϑ, and the fur length parameter δ. The parameter Num_{vertex} is the number of vertex on the fur piece element, which is determined by ξ_i and ρ. φ_l is the random variable of fur length. φ_f is the random variable of relative fineness of fur. φ_θ is the random variable of fur rotation angle. The parameters φ_l, φ_f, and φ_θ are strongly related to the parameter γ in ℓ, that is, the larger the γ is, the broader the range of changes is in φ_l, φ_f, and φ_θ. Fur_{length} is the length parameter on single fur piece element, which is determined by the fur length parameter δ in ℓ and φ_l in ζ. $Fur_{fineness}$ is the fineness parameter of single fur piece element, determined by the density parameter ρ in ℓ, the relative fineness parameter χ, and the parameter φ_f in ζ.

$\psi = \{Cir_i, Tri_i^j : i = 1 \cdots, Z; j = 1, \cdots, Q\}$ is the set of low-level parameters, known as the set of base circle and isosceles triangle. To be specific, each fur piece element contains numbers of fur triangles. The parameter set of each triangle is represented as $Tri_{ij} = \{Tri_{ij}, B_{ij}, B_{ij+1}\}$. T_{ij} is the vertex coordinate of the triangle. B_{ij} and B_{ij+1} are the coordinates of two vertexes at the base of the triangle. The parameter set of each circle is represented as $Cir_i = \{P_i, \xi_i\}$. P_i is the coordinate of the center point of the base circle, ξ_i is the radius of the base circle.

Construction of fur texture model

When building the fur texture model, high-level parameters are sequentially calculated to generate middle-level and low-level parameters. As shown in Figure 6, the main steps of the process are as follows.

Step 1, Set the superposition mode of fur piece elements as the parameter ω, the mathematical definition of ω is shown in Equation (1).

$$\omega = \begin{cases} 0 \text{ coaxial superposition} \\ 1 \text{ off-axis superposition} \end{cases} \tag{1}$$

When the stacking mode is set to coaxial superposition, $\omega = 0$. When the stacking mode is set to off-axis superposition, $\omega = 1$. Taking the off-axis stacking as an example, we first set the coordinate $P_0(x_0, y_0)$ of the center point of the base circle and the coordinate $P_z(x_z, y_z)$ of the center point of the end base circle. Then, we set the spacing parameter ϑ, which could help calculate the coordinate $P_i(x_i, y_i)$ of the base circle's center point of all superimposed piece elements. The calculation formula is shown in Equation (2).

$$\begin{cases} x_i = x_0 + i \cdot \min(\kappa, \vartheta) \cdot \cos\{\arctan[y_z - y_0)/(x_z - x_0)]\} \\ y_i = y_0 + i \cdot \min(\kappa, \vartheta) \cdot \sin\{\arctan[y_z - y_0)/(x_z - x_0)]\} \end{cases} \tag{2}$$

In Equation (2), κ is the restriction factor. In order to prevent the spacing parameter ϑ from being overvalued, we set κ value at 0.05. i represents the number of fur piece elements, $i = 1 \cdots, Z$.

Step 2, set base circle radius ξ and fur length δ. Calculate outer auxiliary concentric circle radius τ_i. We assume that the radius of the base circle of all piece elements are equal, then the formula for the radius τ_i of the outer auxiliary concentric circle is as follows:

$$\tau_i = \xi_i + \delta \tag{3}$$

Centered on P_i, draw the base circle and outer auxiliary concentric circle with radius ξ_i and τ_i. Then, set fur density ρ and fur fineness χ to calculate the number of vertex of triangles on each piece element. After that, set the number of vertex of triangles as Num_{vertex}, the calculation formula is as follows:

$$Num_{vertex} = \text{int}(2\pi \cdot \xi_i \cdot \rho) = Q \tag{4}$$

In Equation (4), Q is represented as the number of vertex of triangles on one single piece element. Based on the number of vertex of triangles, we could calculate the central angle 2θ through the arc $B_{i,j}$ $B_{i,j+1}$, as shown in Equation (5):

$$2\theta = 2\pi / Num_{vertex} \tag{5}$$

Also, we could calculate the width of fur root Λ, the calculation formula of which is shown in Equation (6):

$$\Lambda = 2 \cdot \xi_i \cdot \sin\theta \cdot \chi \tag{6}$$

In Equation (6), the fineness of fur χ is the ratio parameter, and its value range is 20% to 100%.

Step 3, set the vertex coordinate T_i^1 of the triangle right above the center point of the base circle. We could calculate the vertex T_{ij} of the triangle according to the center point coordinate P_i of the base circle, the radius ξ_i of the base circle, the radius τ_i of the outer auxiliary concentric circle, and the center angle θ of the base circle, as shown in Equation (7):

$$\begin{cases} x_{i,j}^r = x_i + \tau_i \cdot \cos(\pi/2 - 2j\theta + 2\theta) \\ y_{i,j}^r = y_i + \tau_i \cdot \sin(\pi/2 - 2j\theta + 2\theta) \end{cases} \tag{7}$$

In Equation (7), i stands for the number of fur piece elements ($i = 1, \cdots, Z$), whereas j represents the number of triangles on each piece element ($j = 1, \cdots, Q$). We could calculate the vertex coordinate B_{ij} of the triangle base, as shown in Equation (8):

$$\begin{cases} x_{i,j}{}^{B} = x_i + \xi_i \cdot \cos\left[\pi/2 - (2j-3)\,\theta - (1-\chi)\,\theta/2\right] \\ y_{i,j}{}^{B} = y_i + \xi_i \cdot \sin\left[\pi/2 - (2j-3)\,\theta - (1-\chi)\,\theta/2\right] \end{cases} \tag{8}$$

As shown in Equation (9), we could also calculate the vertex coordinate $B_{i,j+1}$ of the triangle base.

$$\begin{cases} x_{i,j}{}^{B} = x_i + \xi_i \cdot \cos\left[\pi/2 - (2j-1)\,\theta + (1-\chi)\,\theta/2\right] \\ y_{i,j}{}^{B} = y_i + \xi_i \cdot \sin\left[\pi/2 - (2j-1)\,\theta + (1-\chi)\,\theta/2\right] \end{cases} \tag{9}$$

In Equation (9), when $j = Q$, $B_{i,j+1} = B_{i,1}$.

Step 4, set fur difference parameter γ. Based on γ, we could calculate the random variance of fur length, fur fineness, and the rotation angle of each single fur piece element. What is more, we could represent the random variance of one single piece as $SFL_{i,j}$, where i stands for the number of fur piece elements and j stands for fur quantities. As a result, the random variance matrix φ_l of fur length could be expressed as:

$$\varphi_l = \begin{bmatrix} SFL_{1,1} & \cdots & SFL_{1,j} & \cdots & SFL_{1,Q} \\ \vdots & \ddots & \vdots & \ddots & \vdots \\ SFL_{i,1} & \cdots & SFL_{i,j} & \cdots & SFL_{i,Q} \\ \vdots & \ddots & \vdots & \ddots & \vdots \\ SFL_{z,1} & \cdots & SFL_{z,j} & \cdots & SFL_{z,Q} \end{bmatrix} \tag{10}$$

In Equation (10), $SFL_{i,j} = random\,(-\lambda \cdot \delta/2,\ \lambda \cdot \delta)$, which could take any value between $-\lambda \cdot \delta/2$ and $\lambda \cdot \delta$. The value range of the variance parameter γ is [0, 100%], the greater the value of γ, the larger the change of $SFL_{i,j}$.

If we represent the fineness random variance of one single fur piece as $SFF_{i,j}$, the fineness random variation matrix φ_f in the fur texture model could be expressed as:

$$\varphi_f = \begin{bmatrix} SFF_{1,1} & \cdots & SFF_{1,j} & \cdots & SFF_{1,Q} \\ \vdots & \ddots & \vdots & \ddots & \vdots \\ SFF_{i,1} & \cdots & SFF_{i,j} & \cdots & SFF_{i,Q} \\ \vdots & \ddots & \vdots & \ddots & \vdots \\ SFF_{z,1} & \cdots & SFF_{z,j} & \cdots & SFF_{z,Q} \end{bmatrix} \tag{11}$$

In Equation (11), $SFF_{i,j} = random\,[-\lambda \cdot \chi,\ \lambda \cdot (100\% - \chi)]$, which could take any value between $-\lambda \cdot \chi$ and $\lambda \cdot (1-\chi)$, the larger the value of γ, the greater the variation range of $SFF_{i,j}$.

If we represent the random variable of one single fur piece rotation angle as $SFA_{i,j}$, the fur rotation angle variable matrix φ_θ could be expressed as:

$$\varphi_\theta = \begin{bmatrix} SFA_{1,1} & \cdots & SFA_{1,j} & \cdots & SFA_{1,Q} \\ \vdots & \ddots & \vdots & \ddots & \vdots \\ SFA_{i,1} & \cdots & SFA_{i,j} & \cdots & SFA_{i,Q} \\ \vdots & \ddots & \vdots & \ddots & \vdots \\ SFA_{z,1} & \cdots & SFA_{z,j} & \cdots & SFA_{z,Q} \end{bmatrix} \tag{12}$$

In Equation (12), $SFA_{i,j} = random\,[-\lambda \cdot 2\theta,\ \lambda \cdot 2\theta]$ which could take any value between $-\lambda \cdot 2\theta$ and $\lambda \cdot 2\theta$. When $SFA_{i,j}$ is negative, the triangle on fur piece elements rotates counterclockwise on the base circle. When $SFA_{i,j}$ is positive, the triangle on fur piece elements rotates clockwise on the base circle. The greater the value of γ, the larger the variation range of $SFA_{i,j}$.

Combined with $SFL_{i,j}$ and $SFA_{i,j}$, we could calculate the vertex coordinate $T_{i,j}{}'$ of the triangle after random variation of the fur rotation angle.

$$\begin{cases} x_{i,j}{}^{T'} = x_i + (\tau_i + SFL_{i,j}) \cdot \cos\left[\pi/2 - (2j\theta - 2\theta + SFA_{i,j})\right] \\ y_{i,j}{}^{T'} = y_i + (\tau_i + SFL_{i,j}) \cdot \sin\left[\pi/2 - (2j\theta - 2\theta + SFA_{i,j})\right] \end{cases} \tag{13}$$

Combined with $SFF_{i,j}$ and $SFA_{i,j}$, we could also calculate the vertex coordinates $B_{i,j}{}'$ and $B_{i,j+1}{}'$ of the triangle after random variation of the fur relative fineness, as shown in Equation (14) and Equation (15).

$$\begin{cases} x_{i,j}{}^{B'} = x_i + \xi_i \cdot \cos\left\{\pi/2 - (2j-3)\,\theta - [1-(\chi + SFF_{i,j})]\,\theta/2 + SFA_{i,j}\right\} \\ y_{i,j}{}^{B'} = y_i + \xi_i \cdot \sin\left\{\pi/2 - (2j-3)\,\theta - [1-(\chi + SFF_{i,j})]\,\theta/2 + SFA_{i,j}\right\} \end{cases} \tag{14}$$

$$\begin{cases} x_{i,j+1}{}^{B'} = x_i + \xi_i \cdot \cos\left\{\pi/2 - (2j-1)\,\theta + [1-(\chi + SFF_{i,j})]\,\theta/2 + SFA_{i,j}\right\} \\ y_{i,j+1}{}^{B'} = y_i + \xi_i \cdot \sin\left\{\pi/2 - (2j-1)\,\theta + [1-(\chi + SFF_{i,j})]\,\theta/2 + SFA_{i,j}\right\} \end{cases} \tag{15}$$

Step 5, perform Boolean Operation to obtain the regional elements of star-shaped fur. We fill the gradient from black (at the center of the base circle P_i) to white (at the vertex of triangles $T_{i,j}$), in order to simulate the light decay from the tip to the root of fur. In the strong light environment, we could calculate $Dg_{\max}$ according to the parameter β_+ of light attenuation mitigation, as shown in Equation (16):

$$Dg_{\max} = \tau_i \cdot (1 - \beta_+) \tag{16}$$

Therefore, we could calculate the exact location of the brightness turning point η.

In the weak light environment, we could calculate $Dg_{\max}$ based on the parameter β_- of light attenuation mitigation, as shown in Equation (17):

$$Dl_{\max} = \tau_i \cdot (1 - \beta_-) \tag{17}$$

Therefore, we could figure out the turning point ϖ of brightness.

Based on the five steps mentioned above, we could get the realistic fur texture with dislocated and superposed piece elements. As a result, we could achieve several parametric controls such as superposition mode of fur piece elements, the distance between piece elements, fur length, fur density, fur fineness, fur differences, and fur illumination effect. As shown in Equation (18), the fur element matrix F comprises the radius ξ of base circle, fur length δ, fur density ρ, fur fineness χ, and fur difference γ. Figure 7 shows the shape of fur piece elements under different F effects.

$$F = [\,\xi\ \delta\ \rho\ \chi\ \gamma\,]^{\mathrm{T}} \tag{18}$$

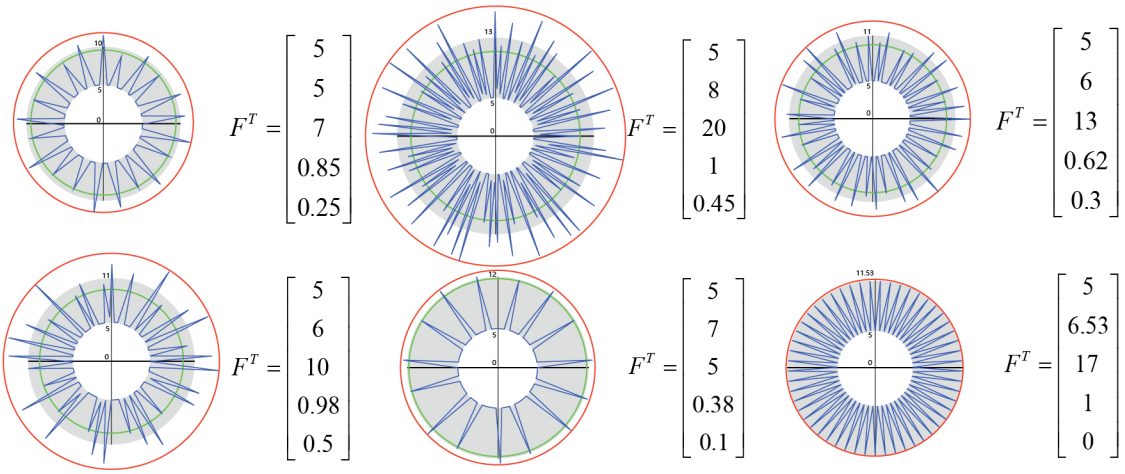

Figure 7. The influence of parameter setting on the geometric contour of fur piece elements

Although parameter values can be set arbitrarily within the value range, different effects on fur simulation result from various kinds of parameter settings such as fur density, fur length, fur fineness, fur diversity, light attenuation, and fur piece element distance. In order to ensure the authenticity of fur, we should take the appropriate value range of each parameter into consideration. Combined with theoretical analysis and experiment research, we could check the value range of each parameter in Table I.

Application

In order to make it easier for designers to adopt the method mentioned above to build a fur texture model, we have explored the possibility of constructing an elemental model of fur piece under the environment of Adobe Illustrator (AI), a general vector drawing software for designers. In AI software, operators could draw various vector graphics by setting the parameters in each dialog boxes. After several experiments, we found out related tools in AI to build the elemental model of fur piece, including star tool, pucker and bloat effect, roughness effect, blend tool, and gradient tool. To be specific, the control parameters in star tool include inner radius of star, outer radius of star, and star angle points. The control parameters in pucker and bloat effect include pucker value and bloat value. The control parameters in roughness effect include roughen size and roughen detail. The control parameter in blend tool includes blend spacing. The control parameters in gradient tool include gradient type and gradient slider location. By analyzing the influence of the parameter changes on the tools mentioned above and comparing the control parameters in the fur texture model, we have established the corresponding relationship between the fur texture model and the parameters in Adobe Illustrator software in Table II.

Table I

Value range of each parameter in fur texture model

Parameter	Value range	Type
Fur density ρ	[10, 30]	Integer
Fur length δ	$[\xi, 4\xi]$	Floating-point
Fur fineness χ	[0.5, 1]	Percentage
Fur diversity γ	[0.2, 0.8]	Percentage
Strong light attenuation mitigation β_+	[0.8, 1]	Percentage
Weak light attenuation mitigation β_-	[0.4, 1]	Percentage
Fur piece element distance ϑ	0.5	Floating-point

Table II

Correspondence between fur texture model and parameters in Adobe Illustrator

Parameters of fur texture model	Related tool in AI	Parameters in AI
The radius of the base circle ξ	Star tool	Inner radius of star
Fur length δ	Star tool	Inner radius of star-Inner radius of star
Fur density ρ	Star tool	Star angle points / 2π Inner radius of star
Fur fineness χ	Pucker & bloat effect	Shrinkage value
Fur diversity γ	Roughen effect	Roughen size
The distance of piece element ϑ	Blend tool	Blend spacing
Strong light attenuation mitigation β_+	Gradient tool	High-brightness gradient slide location
Weak light attenuation mitigation β_-	Gradient tool	Low-brightness gradient slide location

The construction process of fur texture model in AI is shown in Figure 8. First, select a star tool. Set star inner radius, star outer radius and star angle points according to the length and density of fur. Second, use a direct selection tool to round the star's sharp corners, select Pucker & bloat effect, and set shrinkage value of the rounded star according to the relative fineness of fur. Third, select roughness effect. Set roughen size value according to fur variance requirements. Fourth, select gradient tool, set radial gradient from the center of the piece elements to the outermost corner, and set the position of the bright and dark slider according to the light attenuation mitigation. Fifth, replicate and translate fur piece elements. Select blend tool and blend the two piece elements according to the distance of piece elements. Based on the five steps mentioned above, we could produce fur texture realistically based on the dislocated and superposed piece elements.

Results and Discussion

The influence of parameter changes on simulation effect

Based on the method, we could find in Table I that a quite good simulation effect is obtained as long as the distance between piece elements is 0.5mm. Therefore, we should set mixed distance at 0.5mm and star outer radius length at 15mm in AI. The following results show the influence of changes in star angle points, star outer radius length, roughness size, shrinkage value, and slider position on the final simulation effect of fur.

The influence of the star angle points changes on the effect of fur simulation

Set the roughness to 70, the star outer radius length to 30mm, the shrinkage value to -32%, the mixed distance to 0.5mm, the low-brightness slider displacement to 22%, and the high-brightness slider displacement to 100%. By changing the star corner points (SCP), as shown in Figure 9, the picture shows the fur simulation effect at 10, 15, 20, and 25. By contrast, we can find that the more the number of corners, the greater the fur density.

The influence of the star outer radius length change on the fur simulation effect

Set the star angle point to 15, the roughness to 70, the shrinkage value to -32%, the mixed distance to 0.5mm, the low-brightness slider displacement to 22%, and the high-brightness slider displacement to 100%. By changing the star outer radius length (SORL), as shown in

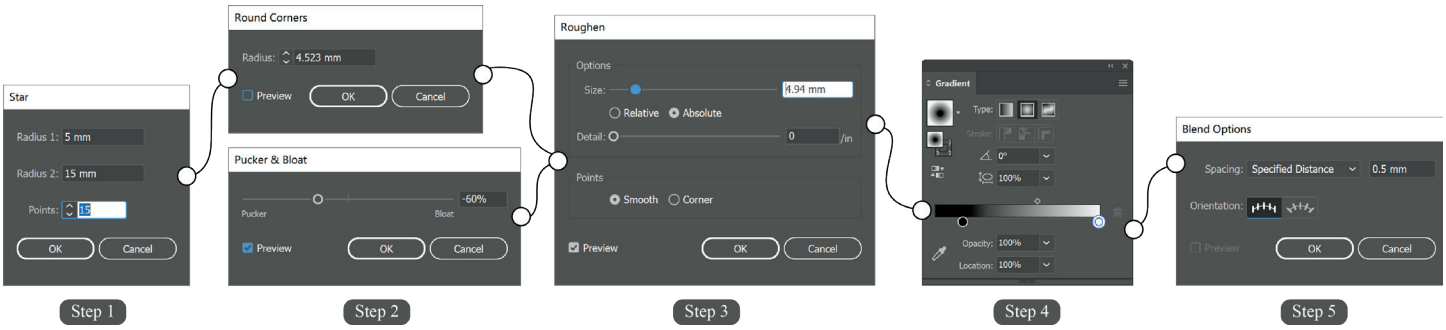

Figure 8. The construction process of realistic fur texture in Adobe Illustrator

Figure 10, the picture shows the fur simulation effect with the outer radius at 35, 40, 45, and 50. By contrast, we can find that the larger the star outer radius length, the greater the fur length.

The influence of the roughness size change on the effect of fur simulation

Set the star angle point to 15, the star outer radius length to 30mm, the shrinkage value to -32%, the mixed distance to 0.5mm, the low-brightness slider displacement to 22%, the high-brightness slider displacement to 100%. By changing the roughness size (RS), as shown in Figure 11, the picture shows the fur simulation effect with the roughness at 20%, 40%, 60%, and 80%. By contrast, we can find that the greater the roughness, the larger the degree of fur differentiation.

The influence of shrinkage value on the effect of fur simulation

Set the star angle point to 15, the star outer radius length to 30mm, the roughness to 70%, the mixed distance to 0.5mm, the low-brightness slider displacement to 22%, and the high-brightness slider displacement to 100%. By changing the shrinkage value (SV), as shown in Figure 12, the picture shows the fur simulation effect with the shrinkage value at -30%, -40%, -50%, and -60%. By contrast, we can find that with the increase of the absolute value of contraction, the density of fur remains the same, and the relative fineness of fur becomes smaller.

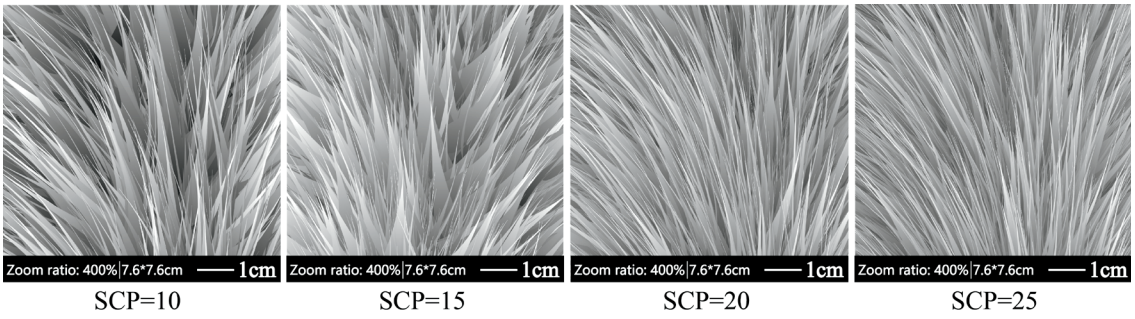

Figure 9. The simulation effect on different star angle points

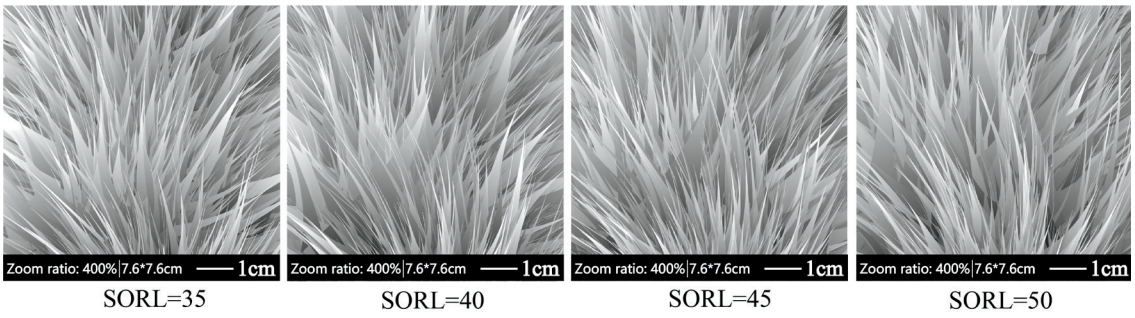

Figure 10. The simulation effect on different star outer radius length

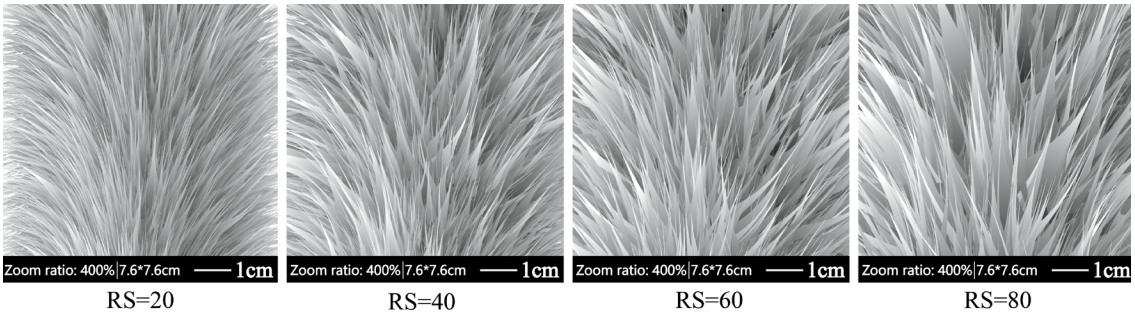

Figure 11. The simulation effect on the change of roughness size

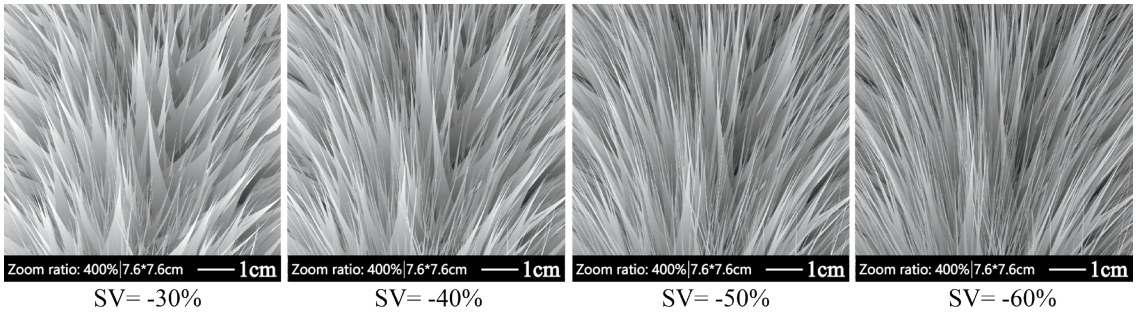

Figure 12. The simulation effect on the change of shrinkage value

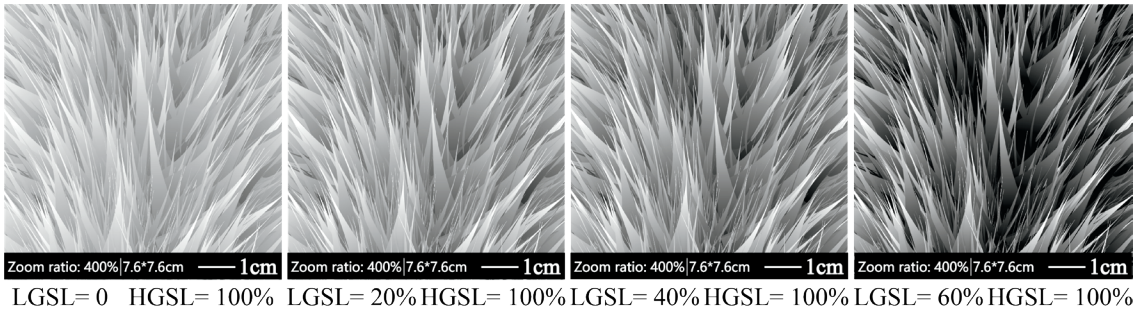

Figure 13. The simulation effect on the location change of the low-brightness gradient slider

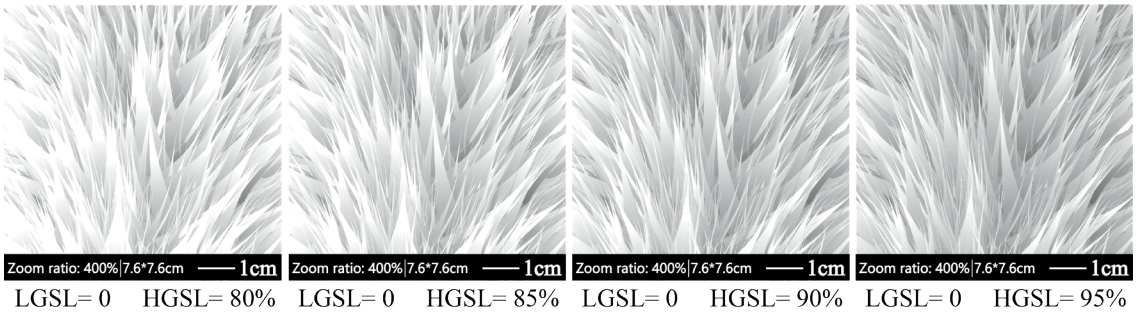

Figure 14. The simulation effect on the location change of the high-brightness gradient slider

The influence of the gradient slider location change on the effect of fur simulation

Set the star angle point to 15, the star outer radius length to 30mm, the roughness to 70%, the mixed distance to 0.5mm, the shrinkage value to -30%, the mode of dislocation and superposition to off-axis dislocation and superposition. By changing the low-brightness gradient slider location (LGSL), as shown in Figure 13, the picture shows the fur simulation effect with the slider location at 0%, 20%, 40%, and 60%. By contrast, we can find that with the increase of the displacement distance of the low-brightness slider, the fur is getting darker. However, by changing the high-brightness gradient slider location (HGSL), as shown in Figure 14, the picture shows the fur simulation effect with the slider location at 80%, 85%, 90%, and 95%. By contrast, we can find that with the increase of the displacement distance of the high-brightness slider, the fur is getting brighter as a whole.

Discussion

The effectiveness of the method

Known from above, we could adjust the parameters to produce fur texture with different length, density, roughness, and illumination performance, representing a perfect sense of reality. As shown in Figure 15, we use basic geometric primitives to form vector fur, so as to possess all the advantages of vector graphics, such as scalability, compatibility, variability, etc.[23]

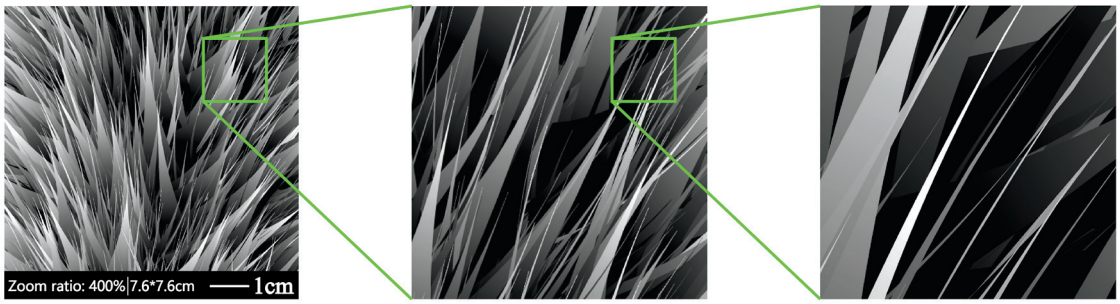

Figure 15. The simulation effect on the magnification factor

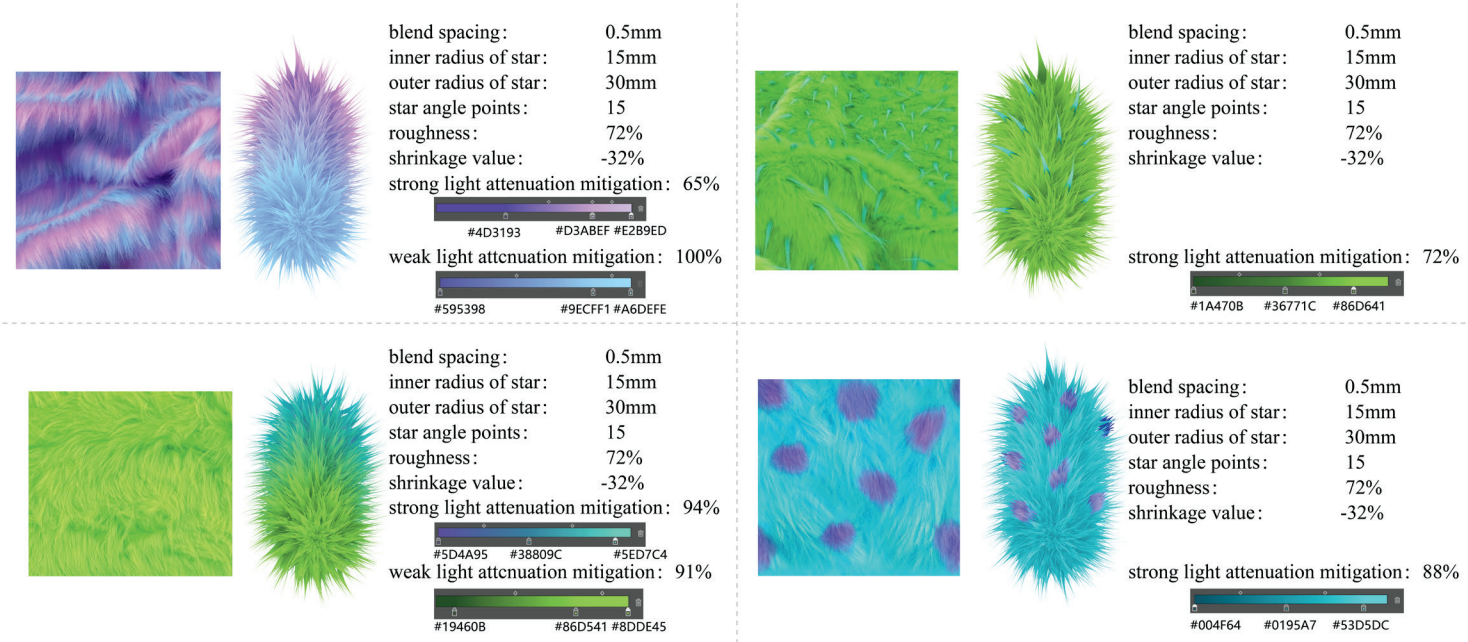

Figure 16. The simulation effects of different kinds of fur

The adaptability of the method

Figure 16 shows the simulation effect of different kinds of fur. Based on the core method of fur piece elements synthesis, we could edit the color of piece elements to generate fur effects with different styles.

Comparisons among the methods

At present, designers use hand-painting, bristle brush, or map rendering to represent fur texture. In this paper, we compared the method of piece-element synthesis with the methods of the bristle brush and the map rendering in many respects, including the advanced principle of fur texture generation, the convenience of user operation, the speed of generation, the rate of modification, the professional requirements of users, and the restrictions on production styles. We can find from Table III that the bristle brush not only lags in the principle of fur texture formation, but also possesses long drawing time and low speed of modification. Even though the map rendering is more advanced in fur texture generation, it is time-consuming and not convenient for designers to operate the software, which seriously impacts efficiency. By comparing the two methods mentioned above, the piece-element synthesis method could not only quickly generate realistic fur texture, but also achieve real-time modification effect by using parameters to control the attributes of fur texture. What is more, designers could promptly visualize fur texture of different kinds of products by implementing the piece-element synthesis method in Adobe Illustrator.

Table III

The comparisons among different fur simulation methods

Category	Bristle brush	Map rendering	Piece-element synthesis
Principles	Updated	Advanced	Advanced
Convenience for operation	Yes	No	Yes
Generation rate	Low	Low	High
Modification rate	Low	Low	High
Requirements for users	Low	High	Low
Restrictions on styles	Low	High	Low

Conclusion

In this paper, a simulation method for realistic fur texture based on the synthesis of piece elements is proposed. In order to better control the geometric details and optical properties of fur model, we defined a parametric model according to dislocation and superposition of fur piece elements. To be specific, we expressed each fur piece element in circle and triangles. Then, we set the fur difference parameter by controlling the hybrid texture of fur and employed the light attenuation mitigation parameter by simulating the light attenuation. Given the two steps mentioned above, we could obtain the realistic fur texture by dislocating and superposing fur piece elements. At the same time, we have verified the feasibility of the matched parameters in Adobe Illustrator software, which could not only simulate the realistic fur texture, but also generate diversified fur in different types. Due to the uncomplicated illumination calculation and low requirements on computer hardware configuration, designers could quickly generate multiple kinds of fur texture by controlling the relevant parameters.

Acknowledgements

This work was financially supported by the Humanities and Social Science Project of Ministry of Education, China (21YJC850013) and Experimental Technology Program of Sichuan University (SCU201134). The authors acknowledge Siyuan Li for her contribution to grammar corrections.

References

1. Lengyel, J., Praun, E., Finkelstein, A., et al.; Real-time fur over arbitrary surfaces. *Proceedings of the 2001 symposium on Interactive 3D graphics,* 227-232, 2001.
2. Thalmann, N.M., Carion, S., Courchesne, M., et al.; Virtual clothes, hair and skin for beautiful top models. *IEEE,* 132-141, 1996.
3. Szajerman, D. and Jurczyński, A.; Fur visualisation for computer game engines and real-time rendering. *International Conference on Computer Vision and Graphics,* 41-48, 2014.
4. Goldman, D.B.; Fake fur rendering. *Proceedings of the 24th annual conference on Computer graphics and interactive techniques,* 127-134, 1997.
5. Angelidis, A. and McCane, B.; Fur simulation with spring continuum. *The Visual Computer* **25**, 255-265, 2009.
6. Kowalski, M.A., Markosian, L., Northrup, J.D., et al.; Art-based rendering of fur, grass, and trees. *Proceedings of the 26th annual conference on Computer graphics and interactive techniques,* 433-438, 1999.
7. Csuri, C., Hackathorn, R., Parent, R., et al.; Towards an interactive high visual complexity animation system. *Acm Siggraph Computer Graphics* **13**, 289-299, 1979.
8. Miller, G.; From wire-frames to furry animals. *Graphics Interface,* 138-145, 1988.
9. LeBlanc, A.M., Turner, R., and Thalmann, D.; Rendering hair using pixel blending and shadow buffers. *The Journal of Visualization and Computer Animation* **2**, 92-97, 1991.
10. Watanabe, Y. and Suenaga, Y.; A trigonal prism-based method for hair image generation. *IEEE Computer Graphics and applications* **12**, 47-53, 1992.

11. Gelder, A.V. and Wilhelms, J.; An interactive fur modeling technique. *Graphics Interface,* **97**, 181-188, 1997.
12. Reeves, W.T.; Particle systems-a technique for modeling a class of fuzzy objects. *ACM Transactions on Graphics (TOG)* **2**, 91-108, 1983.
13. Perlin, K.; Hypertexture. *Proceedings of the 16th annual conference on Computer graphics and interactive techniques,* 253-262, 1989.
14. Kajiya, J.T. and Kay, T.L.; Rendering fur with three dimensional textures. *Computer Graphics* **23**, 271-280, 1989.
15. Meyer, A. and Neyret, F.; Interactive volumetric textures. *Eurographics Workshop on Rendering Techniques,* 157-168, 1998.
16. Lengyel, J.E.; Real-time fur. *Eurographics Workshop on Rendering Techniques,* 243-256, 2000.
17. Kazuya, S., Naomi, I., and Hiroko, S.; Handling evaluated by visual information to consider web-consumers. *International Journal of Clothing Science and Technology* **16**, 153-162, 2004.
18. Dana, K.J., Van Ginneken, B., Nayar, S.K., et al.; Reflectance and texture of real-world surfaces. *ACM Transactions on Graphics (TOG)* **18**, 1-34, 1999.
19. Ling, Q.Y., Tseng, C.W., Jensen, H.W., et al.; Physically accurate fur reflectance: Modeling, measurement and rendering. *ACM Transactions on Graphics (TOG)* **34**, 1-13, 2015.
20. Marschner, S.R., Jensen, H.W., Cammarano, M., et al.; Light scattering from human hair fibers. *ACM Transactions on Graphics (TOG)* **22**, 780-791, 2003.
21. Andersen, T.G., Falster, V., Frisvad, J.R., et al.; Hybrid fur rendering: combining volumetric fur with explicit hair strands. *The Visual Computer* **32**, 739-749, 2016.
22. Jiang, H., Zhou, M., Wu, Z., et al.; Survey of appearance models and rendering. *Computer science* **41**, 1-7, 2014.
23. Wang, W., Wang, W., Peng, B., et al.; Simulating the surface of litchi grain leather by creating quadrilateral-continuous pattern in Adobe Illustrator CC. *Leather and Footwear Journal* **19**, 51-60, 2019.

Effect of Enzymatic Treatment in Leather Manufacture at Different Processing Stage

by

Jayakumar GC,[1,4] Karthik V,[2] Jeyas Kandhan S[1,4] and Kanagaraj J[3,4]

[1]*Centre for Academic and Research Excellence*

[2]*Regional Centre*, Jalandhar

[3]*Leather Process Technology Department, CSIR-Central Leather Research Institute*, Adyar Chennai, India

[4]*Department of Leather Technology, Alagappa College of Technology, Anna University*, Chennai

Abstract

The use of cleaner leather processing technologies is of great interest today due to the global trends favoring environmentally friendly manufacturing. Modernization and implementation of new technologies, like enzyme-driven catalysis instead of conventional inorganic catalysis, can improve the quality and reduce the cost of leather manufacturing while making the leather more environmentally sustainable. The use of enzymes in pre-tanning operations is a well-known technology. However, a holistic view of the effect of enzymes at various stages of leather processing is limited. We attempt to bridge this gap by studying the influence of enzymes on the characteristics of crust leather at multiple locations of leather processing. Trypsin was used to assess the enzymatic action on delimed pelts, while pepsin was used to evaluate the impact of enzyme treatment on a pickled pelt that was later chrome tanned.

Similarly, papain was used to study enzymatic activity on neutralized, chrome-tanned leather. The selection of enzymes for three different materials was guided by the optimal activity behavior of the enzymes. It is observed that the physical strength characteristics of the enzyme-treated leathers show minor differences. Hence, this study aims to explore the unconventional application of enzymes at various stages of leather processing.

Introduction

The leather industry is a traditional manufacturing sector but one that constantly adopts newer technologies to achieve sustainability.[1] The invention and implementation of cleaner technologies are essential to meet new environmental norms and meet the ever-changing requirements of consumers. Several cleaner practices including zero liquid discharge, effluent treatment through various techniques, mineral-free tanning systems, high exhaust tanning systems, aldehyde-free syntans, enzyme-assisted beam house operations, natural dyes, solvent-free finishing systems, etc. have been reported.[2-10] Of all clean manufacturing practices, enzyme-assisted processing has always been an exciting topic of study for the leather fraternity. Enzyme-assisted unhairing, fiber opening, defleshing, and scuds removal are processes where hydrolytic enzymes have been used. Proteases, amylases, and lipases are the most widely used classes of enzymes in leather processing for unhairing, fiber opening, and defleshing, respectively.[11-14] The use of protein-digesting enzymes (proteolytic enzymes) during leather processing to remove unwanted proteins other than collagen is also common. In this study, proteolytic enzymes of different specificities and functions, trypsin, pepsin, and papain, have been employed. Pepsin is an aspartic protease, while trypsin is a serine protease. Papain, a well-reported enzyme in leather processing, is very active in the neutral pH range, whereas pepsin and trypsin are in acidic and basic pH ranges respectively. The present study discusses the effect of enzymatic treatment on delimed pelt, pickled pelt, and chrome tanned leather using trypsin, pepsin, and papain, respectively.[15] The study is exploratory, and the characteristics of enzyme-treated crust leather were evaluated using a combination of tensile testing, grain crack measurement, and microscopic imaging.

Materials and Methods

Materials and Chemicals

All leather chemicals were of commercial-grade, and analysis chemicals were of analytical grade. The raw material used for leather processing was wet salted goat skins. Leather processing trials are detailed in Tables I-III.

Table I

Process Recipe for Trypsin Treatment

Process	Conc.	
Delimed Pelt		
Water	100%	
Trypsin	**0-1.0%**	**45-60 min**
Washing I	100	15 min
Washing II	100	15 min
Pickling		pH 2.8-3.0
Chrome Tanning	6%	
Basification		pH 3.8-4.0

*Corresponding author email: jaykumar@clri.res.in

Manuscript received March 12, 2022, accepted for publication July 30, 2022.

Table II

Process Recipe for Papain Treatment

Process	Conc	
Chrome tanned leather		
Neutralization		pH 5.5-6.0
Papain	**0-1.0%**	**45-60 min**

Table III

Process Recipe for Pepsin Treatment

Process	Conc	
Delimed Pelt		
Pickling		pH 2.8-3.0
Pepsin	**0-1.0%**	**45-60 min**
Chrome Tanning	6%	
Basification		pH 3.8-4.0

Table IV

Process Recipe for Post Tanning

Process	Chemicals	% of Chemicals	Duration (min)	Remarks
Wet Back and Acid Wash	Water	100		
	Acetic Acid	0.5		
	Wetting Agent	0.5	30	Adjust pH 2.8-3.0
Rechroming	Water	100		
	BCS	4		
	Cr. Syntan	4		
	Acrylic Syntan	2		
	Fish Oil F/L	1	40	
Basification	Water	100		
	Sodium Formate	0.5		
	Sodium Bicarb	0.5	2 × 10 + 20	Adjust pH 3.8-4.0
Neutralisation	Water	100		
	Neut. Syntan	2	20	
	Sodium formate	2	20	Adjust pH 5.5-6.0
		Drain / Wash / Drain		
Retanning	Water	100	20	
	Acrylic Syntan	2		
	SMA Syntan	2	30	
	Polymeric/Phenolic Syntan	3		
	Melamine Based Syntan	2		
	Fillers	2		
	Wattle GS	2		
	Synthetic F/L	1	60	
Dyeing	Anionic Dye	X	30	
Fatliquoring	Water	100		
	Synthetic Fatliquor	2		
	Polymeric / Semi-Synt F/L	2		
	Veg based F/L	1		
	Fish Oil F/L	1		
	Preservative	0.1	60	
Fixing	Formic Acid	3	3 × 5' + 30	
Top Fatliquoring	Cationic F/L	1	20	
		Drain / Wash / Drain		

Physical testing of leather samples

The samples for physical testing were obtained as per IULTCS methods.[16] The samples were conditioned at 26°C and 65% R.H. for 48 hours. Tensile strength[17] and grain crack[18], were measured as per standard procedures.

Microscopic Evaluation

Scanning electron microscopic techniques were used to understand the grain and surface characteristics of the leathers.

Determination of Hydroxyproline

To determine the effect of enzymes on collagen fibers, hydroxyproline content was estimated in the processed liquor using Woessner's method.[19] The quantity of hydroxyproline present was calculated by using the standard equation obtained by plotting standard curve.

Result and Discussion

Enzymatic processing is gaining interest owing to its cleaner manufacturing methods. Conventionally, proteases, amylases and lipases are the three enzymes used in the pretanning process. However, the influence of the enzyme on the skins at different processing stages is less explored and recently use of elastase in wet end processing was found to enhance area yield.[20] In the present study, three model enzymes were chosen to understand the leather Characteristics, viz., Trypsin on delimed pelt; Pepsin on the pickled pelt and papain on the chrome tanned leather. The selection of enzymes and the suitable substrate have been chosen based on the optimum enzyme activity. Enzymatic treatment of all the three enzymes on the skins has been studied as given in Table I-III. For Pepsin and Trypsin trials, conventional chrome tanning and post tanning have been carried out as given in Table IV after the enzymatic treatment. Whereas, for papain trials, after enzymatic treatment, the post-tanning process has been carried out at pH 5.5-6.0, as given in Table IV. After completing the post-tanning processes, the leather was tested for its physical strength properties, and the leather images are shown in Figure 1.

The images of processed crust leathers are shown in Figure 1. The leathers are found to be smoother with higher concentration of enzymatic treatment in all the trials. This might be due to the enzyme activity on the fibers which aids in smooth characteristics. Moreover, leathers are found to be soft in the enzyme treated trials.

Topological Images of the Enzyme Treated Crust Leather

The SEM images of the control post tanned leather and the experimental post tanned leather using 1% trypsin on delimed pelt, 1% pepsin on the pickled pelt and 1% papain on the chrome tanned leather are shown in the Figure 2, 3 and 4 respectively.

Papain-Neutral pH	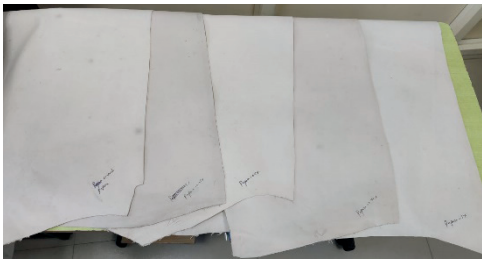
Pepsin-Acidic pH	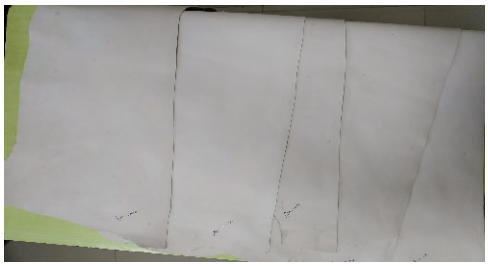
Trypsin-Alkali pH	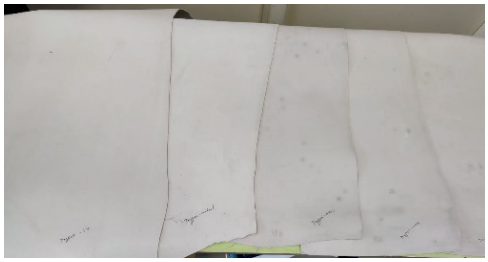

Figure 1. Images of enzymatic treated post tanned leathers

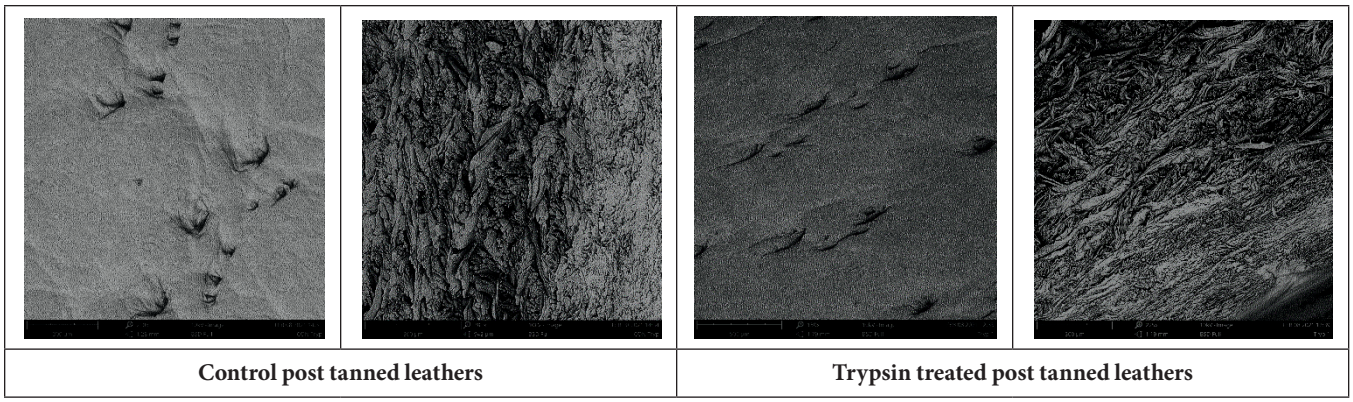

Figure 2. SEM images of control and trypsin treated crust leathers

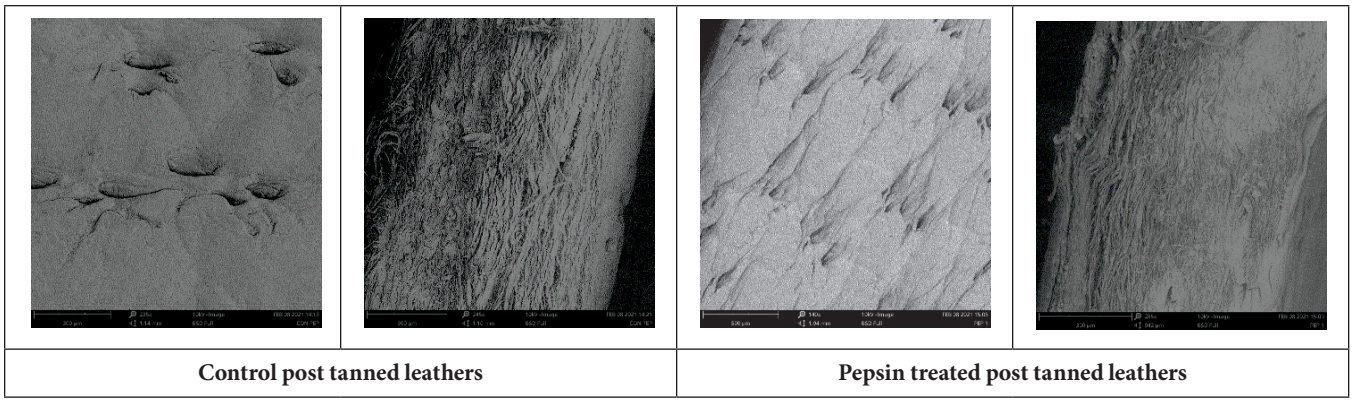

Figure 3. SEM images of control and pepsin treated crust leathers

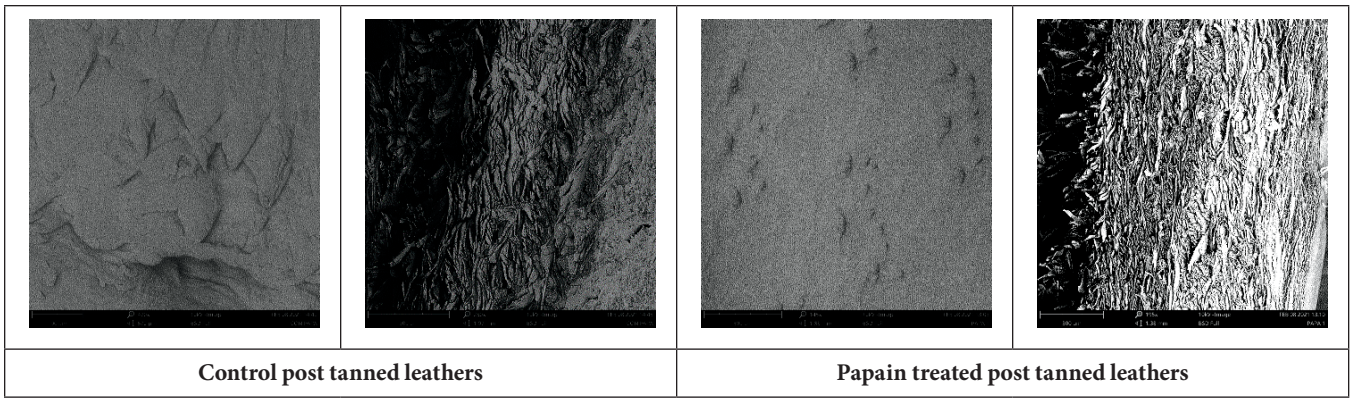

Figure 4. SEM images of control and papain treated crust leathers

The micrographic images of the crust leathers (Grain surface and Cross section) are shown in the Figure 2-4. Cross section images of the control and experimental leathers are found to be similar. Moreover, there is no disfigurement have been inferred on the grain surface due to enzymatic treatments.

Physical characteristics of the crust leather

The physical characteristics such as tensile strength and the tear strength were determined for the enzyme treated leathers and the results are given in the Table V-VII.

The pepsin treated crust leather has shown some varying result. The use of 0.25% and 1.0% of enzyme has shown a decrease in strength properties.

Treatment of trypsin on the delimed pelt has given a variation in strength characteristics. However, the tear strength has been reduced by the trypsin treatment with respect to the conventional processed crust leather.

The papain treated crust leather has also shown some varying result. The concentration of papain at 0.50% on the chrome tanned leather has shown a significant enhancement in the strength characteristics,

Table V

Pepsin treated crust leather physical characteristics

S. No.	Enzyme %	Tensile Strength (MPa)	Tear Strength (N/mm)
1.	0.25	24	66
2.	0.50	37	90
3.	0.75	38	104
4.	1.00	28	63
5.	Control	33	64

Table VI

Trypsin treated crust leather physical characteristics

S. No.	Enzyme %	Tensile Strength (MPa)	Tear Strength (N/mm)
1.	0.25	35.9375	79.5825
2.	0.50	38.0225	105.1275
3.	0.75	36.4725	80.3875
4.	1.00	38.175	110.835
5.	Control	37.5425	131.8175

Table VII

Papain treated crust leather physical characteristics

S. No.	Enzyme %	Tensile Strength (MPa)	Tear Strength (N/mm)
1.	0.25	29	91
2.	0.50	44	136
3.	0.75	36	83
4.	1.00	38	117
5.	Control	38	117

while the use of 0.25% and 0.75% of enzyme has shown decreased strength properties.

Grain crack properties

The crust leather treated with the enzymes were subjected to the lastometer test to determine the grain crack properties and the results are given in the Table VIII-X.

From the results (Table VIII-X), it can be established that enzymes have influenced the grain surface on the leathers, enzyme treated leathers have shown lesser distention at grain crack as compared to the control leathers. However, 0.5% papain treated leathers have higher distention grain crack which is in accordance with the higher strength properties of the leathers.

Table VIII

Lastometer test for pepsin treated leather

S. No.	Enzyme %	Load at Grain Crack (Kg)	Distention at Grain Crack (mm)
1.	0.25	45.91	7.95
2.	0.50	54.94	7.52
3.	0.75	50.1	7.26
4.	1.00	36.62	7.56
5.	Control	54.55	8.03

Table IX

Lastometer test for trypsin treated leather

S. No.	Enzyme %	Load at Grain Crack (Kg)	Distention at Grain Crack (mm)
1.	0.25	56.42	7.78
2.	0.50	64.42	8.09
3.	0.75	61.69	7.71
4.	1.00	73.86	8.32
5.	Control	80.04	7.92

Table X

Lastometer test for papain treated leather

S. No.	Enzyme %	Load at Grain Crack (Kg)	Distention at Grain Crack (mm)
1.	0.25	48.80	7.50
2.	0.50	78.05	8.76
3.	0.75	53.41	7.47
4.	1.00	43.48	7.58
5.	Control	49.45	7.36

Hydroxyproline assay

To assess the impact of enzymes on collagen, hydroxyproline assay was carried out separately for the liquors collected during leather processing treated with respective enzymes. The hydroxyproline estimation helps us to understand whether the collagen structure is damaged and indicates impairment in mechanical strength of leather.

The hydroxyproline results were given in table XI. Based on the results obtained, it has been observed that papain did not have any kind of impact on collagen fiber. Whereas, the trypsin and pepsin at the concentration of 0.25% and 0.5% did not show any hydroxyproline release. Although, when the concentration of trypsin and pepsin was increased, there was an increment in the hydroxyproline release. However, the release of hydroxyproline depends on several factors such the substrate, temperature and duration.

Significance of Enzymatic Treatment

Enzyme driven leather processing technologies gains significant attention amidst leather manufacturing owing to eco-acceptance. Conventionally as shown in Figure 5, enzymes have been used in the bating operation to remove scuds and open up the fiber bundles for better exhaustion of chemicals. However, the present research focused on using unconventional enzymes in leather to enhance the physical properties of the leathers. Leathers treated with enzymes have shown smoothness in grain as compared to the control process. Similarly, enzyme treated leathers were more pliable than the control processed leathers. Though, tanned leathers show resistance to the enzymatic treatments, however from the current research it is evident that fiber relaxation can be achieved using enzymes which enhances the smoothness and pliable properties of the leathers.

Conclusion

Enzymatic processing is a way forward towards cleaner and sustainable leather processing method. The present research focused on understanding the influence of enzymes at varied leather processing stages and corroborate with the strength characteristics

Table XI

Hydroxyproline Assay for liquor collected during leather processing treated with respective enzymes

	Hydroxyproline (µg/mL)			
S No	**0.25%**	**0.5%**	**0.75%**	**1%**
Trypsin	0	0	2.023	5.745
Papain	0	0	0	0
Pepsin	0	0	1.518	2.641

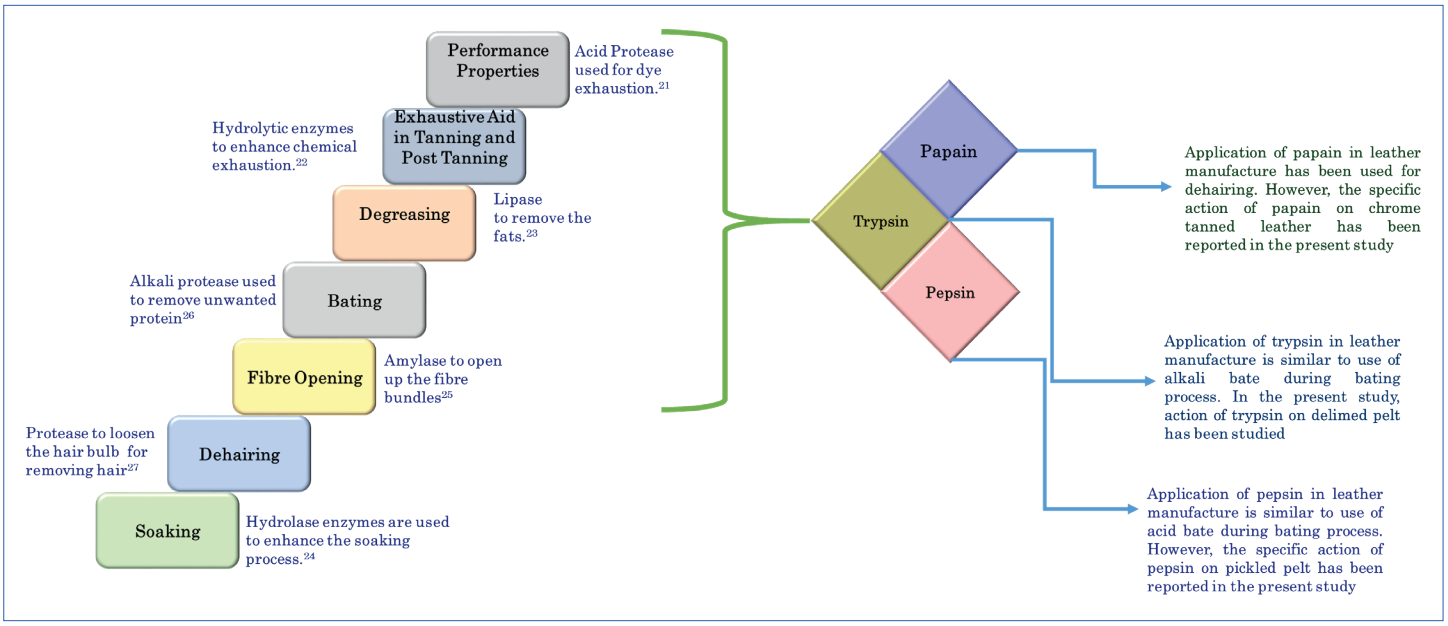

Figure 5. Significance of enzyme in leather manufacture

of the crust leathers. Influence of protease, amylase and lipase have been well reported on the leather characteristics. However, unconventional enzymes like pepsin and trypsin impact on leather have been reported in this study. Moreover, enzymes are also looked upon as an auxiliary aid to improve exhaustion of chemicals to endorse that this study would provide an insight on the strength properties.[21] The results have shown there is no significant influence on the strength properties, whereas there is marginal decrease in the distention at grain crack which is possibly due to the enzymatic interaction on the grain surface which in turn provides the smooth surface to the experimental leathers.

Acknowledgements

Authors would like to thank the Director, CSIR-CLRI and CLRI-CATERS for facilitating the testing facilities. Authors also acknowledge the financial support from CSIR funded project Innovative Fundamental Research for attaining Sustainability in Leather Sector (IFRES), MLP2004. CSIR-CLRI communication is 1744.

References

1. Ramchandani M, Coste-Maniere I.; Leather in the Age of Sustainability: A Norm or Merely a Cherry on Top? Muthu S. (eds) Leather and Footwear Sustainability. *Textile Science and Clothing Technology*, 11-22, 2020.
2. Azhar Alia, Irfan Ahmed Shaikha, Naeem Akhtar Abbasia, Nabeela Firdousa, Muhammad Naveed Ashraf; Enhancing water efficiency and wastewater treatment using sustainable technologies: A laboratory and pilot study for adhesive and leather chemicals production. *Journal of Water Process Engineering*, **36** (101308), 2020.
3. Sundar V J, Muralidharan C.; An Environmentally Friendly Mineral-Free Tanning of Animal Skins – Sustainable Approach with Plant Resources. *Environ. Process.* **7**, 255–270, 2020.
4. Sundar V J, Raghava Rao J, Muralidharan C.; Cleaner chrome tanning — emerging options. *Journal of Cleaner Production*, **10** (1), 69-74, 2002.
5. Josep M.Morera, Anna Bacardit, Lluís Ollé, Esther Bartolí, Maria D.Borràs; Minimization of the environmental impact of chrome tanning: A new process with high chrome exhaustion. *Chemosphere*, **69** (11), 1728-173, 2007.
6. Xinhua Liu, Youyou Wang, Xuechuan Wang and Huie Jiang; Development of hyperbranched poly-(amine-ester) based aldehyde/chrome-free tanning agents for sustainable leather resource recycling. *Green Chem*., **23**, 5924-5935, 2021.
7. Aravindhan A, Madhan B, Raghava Rao J.; Studies on Tara-phosphonium Combination Tannage: Approach Towards a Metal Free Eco-Benign Tanning System. *JALCA* **110** (03), 2015.
8. Kurinjimalar C, Jayakumar GC, Tamil Selvi A, Venba R, Malathy J, Swarna V Kanth; Biocolorant for Leather Dyeing Applications: An Eco-benign Evaluation of Natural Coloring Agent. *JALCA* **116** (9), 2021.
9. Yang, Z., Zang, H. & Wu, G.; Study of solvent-free sulfonated waterborne polyurethane as an advanced leather finishing material. *J Polym Res*, **26**, 213, 2019.
10. Zhimeng Liu, Bo Wu, Yuanyuan Jiang, Jingxin Lei, Changlin Zhou, Junhua Zhang, Jiliang Wang; Solvent-free and self-catalysis synthesis and properties of waterborne polyurethane. *Polymer*, **143**, 129-136, 2018.
11. Jayakumar GC, Sathish M, Aravindhan R, Raghava Rao J.; Studies on the use of bi-functional enzyme for leather making. *JALCA* **111**, 455-460, 2016.

12. Gunavadhi M, Jamal ZM, Jayakumar GC, Yasmin K, Sreeram KJ, Raghava Rao J.; A novel approach to enzymatic unhairing and fibre opening of skin using enzymes immobilized on magnetite nanoparticles. *ACS Sustainable Chem. Eng.*, **4** (3), 828–834, 2016.
13. Jayakumar GC, Sivaraman G, Mohan R, Saravanan P, Raghava Rao J.; Cohesive system for enzymatic unhairing and fibre opening: Architecture towards Eco-benign pretanning operation. *Journal of Cleaner Production*, **83**(8), 428-436, 2014.
14. Gunavadhi M, Mohammad Jamal Azhar Zakir, GC Jayakumar, K Yasmin, KJ Sreeram, J Raghava Rao; A Novel Approach to Enzymatic Unhairing and Fiber Opening of Skin Using Enzymes Immobilized on Magnetite Nanoparticles. *ACS Sustainable Chem. Eng.*, **4** (3), 828–834, 2016.
15. R B Choudhary, A K Jana & M K Jha; Enzyme technology applications in leather processing. *Indian Journal of Chemical Technology.* **11**, 659-671, 2004.
16. IUP 2, Sampling, *JSLTC*, **84**, 303, 2000.
17. IUP 6, Measurement of tensile strength and percentage elongation, *JSLTC* **84,** 317-321, 2000.
18. SLP 9 (IUP 9), Measurement of Distension and Strength of Grain by the Ball Burst test, Official methods of analysis.
19. Woessner Jr, J. F.; The determination of hydroxyproline in tissue and protein samples containing small proportions of this imino acid. *Archives of biochemistry and biophysics*, **93**(2), 440-447, 1961.
20. Novocor AX, Elastase-Active Enzymes, Granulate, Novozymes
21. Swarna VK, Venba R, Jayakumar GC, Chandrababu NK. Kinetics of leather dyeing pretreated with enzymes: Role of acid protease. *Bioresource Technology*, **100**(8), 2430-2435, 2009.
22. Md Jawad Hasan, Papia Haqueb, Mohammed Mizanur Rahman; Protease enzyme based cleaner leather processing: A review. *Journal of Cleaner Production*, **365**, 2022.
23. Altan A, Fatma Ç.; A Research on Increasing the Effectiveness of Degreasing Process by Using Enzymes. *Textile and Apparel*, **18** (4), 278, 2008.
24. Jianzhong Ma, Xueyan Hou, Dangge Gao, Bin Lv, JingZhang; Greener approach to efficient leather soaking process: role of enzymes and their synergistic effect. *Journal of Cleaner Production,* **78**, 226-232, 2014.
25. Subramani Saravanabhavan, Rathinam Aravindhan, Palanisamy Thanikaivelan, Jonnalagadda Raghava Rao and Balachandran Unni Nair.Green; Solution for tannery pollution: effect of enzyme-based lime-free unhairing and fibre opening in combination with pickle-free chrome tanning. *Green Chemistry*, **5**, 707–714, 2003.
26. Hameed A, Natt M.A and Evans C.S.; Production of alkaline protease by a new Bacillus subtilis isolate for use as a bating enzyme in leather treatment. *World Journal of Microbiology & Biotechnology*, **12**, 289–291, 1996.
27. Aline Dettmer, Élita Cavalli, Marco A.Z. Ayub and Mariliz Gutterres; Environmentally friendly hide unhairing: enzymatic hide processing for the replacement of sodium sulfide and deliming. *Journal of Cleaner Production*, **47**, 11-18, 2013.

Lifelines

Chunxiao Zhang see *JALCA* **114**, 189, 2019

Buqing Ye is a postgraduate student at Sichuan University, China. Her research work focuses on resource utilization of animal skins/hides solid waste. She is under the guidance of Dr. Chunxiao Zhang.

Jinzhi Song is a Ph. D. student at Sichuan University, China. She is working at bio-technology of leather-making. She is under the guidance of Prof. Biyu Peng.

Biyu Peng see *JALCA* **109**, 207, 2014

Alireza Koochakzaei is an assistant professor of archaeometry and conservation of historic and cultural properties at Tabriz Islamic Art University, Tabriz, Iran. He received a BA in art conservation from University of Zabol and an MA and Ph.D. in conservation of cultural and historic properties from Art University of Isfahan. He was selected as the top student in the country (Iran 2017). He has worked as a lecturer at the Art University of Isfahan and a conservator in the archaeological museum of Birjand (south Khorasan province of Iran). His scientific interests are mainly focused on the conservation of artifacts made from organic materials, especially leather. Currently, he is researching leather treatment methods and the conservation of acid-deteriorated leathers. He is also interested in the development and application of spectroscopy methods for archaeometry, conservation purposes and the evaluation of biodeterioration and degradation mechanisms in historical objects made from organic materials.

Mohammad-Amin Sabaghian Bidgoli is an M.A. in archaeometry. He received a BA in art conservation and an M.A. in archaeometry from Tabriz Islamic Art University.

Siyamak Safapour obtained his Ph.D. and master's degree in Textile Chemistry and Fiber Science Engineering at Amirkabir University of Technology, Tehran, Iran. He is currently an associate professor at Tabriz Islamic Art University. His main research interests are the development of green chemistry and technologies in textiles processing; Isolation, characterization, and application of natural dyes and pigments; Green synthesis of metal nanoparticles for textiles applications; Green coloration and functional finishing of natural and synthetic textiles; Synthesis, characterization, and application of novel functional textile dyes (antibacterial, UV-Protective, antioxidant, insect repellent, etc.); Surface modification of textile fibers.

Wei Wang received his Master's Degree (2012) in Fashion Design and Engineering from Sichuan University, China. Then he works in the Department of Fashion Design at Sichuan University. He was a visiting scholar at Birmingham City University, UK, from 2015 to 2016. Now he is a Ph.D. candidate in the National Engineering Research Center of Clean Technology in Leather Industry, Sichuan University, China. Recently, his research work mainly focuses on leather product engineering and materials.

Weijie Wang received his Master's Degree (2019) in Fashion Design and Engineering from Sichuan University, China. He is now a Ph.D. candidate in the College of Biomass Science and Engineering, Sichuan University, China. Recently, his research work mainly focuses on digital fashion design and wearable electronics.

Gaopeng Zhang is an Associate Professor in the Department of Fashion Design at Sichuan University. Besides regular teaching in courses in Apparel CAD, Design Management and Chinese Ethnic Costume, he retains a keen interest in the studies of apparel technologies, fashion design management, and fashion popularity and sociocultural development.

Luming Yang received her Master's Degree (2004) in Leather Chemistry and Engineering from Sichuan University, China, and the Ph.D. (2007) in Chemistry and materials technology from Tomas Bata University in Zlin, Czech. Now she is a Professor in the Department of Fashion Design, Sichuan University, China. Her broad research fields are functional and intelligent clothing design, footwear and health, foot biomechanics, with a particular focus on functional clothing and sports biomechanics.

Biyu Peng see JALCA 109, 207, 2014

G.C. Jayakumar is Senior Scientist at Centre for Academic and Research Excellence, CSIR-Central Leather Research Institute, Chennai, India. His research interests include cleaner leather

processing technologies and utilization of tannery wastes for developing products.

V. Karthik is Senior Scientist at Regional Centre - Jalandhar, CSIR-Central Leather Research Institute, Chennai, India. His research interests include leather processing technologies and evaluation of leather.

S. Jeyas Kandhan is currently a Post Graduate Student of Leather Technology at the Department of Leather Technology, AC Tech Campus, Anna University housed at CSIR-Central Leather Research Institute, Chennai, India. His research interests include biotechnological aspects of leather processing and waste management system in the leather industry.

J. Kanagaraj is Chief Scientist at Leather Process Technology Department, CSIR-Central Leather Research Institute, Chennai, India. His research interests include cleaner leather processing technologies, development of curing and tanning technology and tannery solid waste management.

Journal Publication Policy

1 - Submission

Manuscripts, which meet the following requirements, should be submitted in electronic format to: **jalcaeditor@gmail.com** as a single Word e-mail attachment (including embedded Figures and Tables in JPG and/or Excel).

2 - Subject Matter

The *Journal of the American Leather Chemists Association* publishes manuscripts on all aspects of leather science, engineering, technology, and economics, and will consider related subjects that address concerns of the industry. Examples: hide/skin quality or utilization, leather production methods/equipment, tanning materials/leather chemicals, new and improved leathers, collagen studies, leather by-products, impacts of changes in leather products industries, process efficiency, sustainability, regulatory, safety, environmental, tannery waste management and industry economics.

3 - Types of Articles

Four categories articles are considered: **Technical Papers, Technical Notes, Reviews and Invited Lectures.**

Our major publication emphasis, **Technical Papers**, should be a thorough treatment of a specific subject, including such figures and tables (F&T) necessary to illustrate the points made in the text and to justify the conclusions drawn. Technical Papers are subject to peer review prior to acceptance.

Technical Notes accommodate less formal presentations from the tanning industry and suppliers, especially those made at the Association's annual meetings. Notes from the supplier industries should include technical data to justify the statements made. Notes, while less formal, must meet the literary standards of the *Journal*, but need not contain an experimental section or references and are usually not Peer Reviewed.

Review Papers and **Invited Lectures** will be published only on currently important theoretical or practical aspects of leather science, manufacture, and economics and must meet *Journal* literary standards.

4 -General Requirements for Manuscripts

English Language: Manuscripts must be submitted in native American English language consistent with *Journal* standards and sufficient to enable Peer Review of technical content.

The **First page** should have a running head, title, authors' last names with initials, (corresponding author footnoted with e-mail address) and authors' affiliations/addresses. Also footnote occasion, place and date of presentation on which the paper is based if appropriate.

While some formatting flexibility is permitted, it is recommended that **Technical Papers** be submitted with the following sections:

- **Abstract** Tells why the work was done and may generally state results (minimize data details) and their significance in one paragraph.
- **Introduction** Must judiciously reference using superscripts (ex…word.[6,7]) the important contributions to the subject that have been previously published, clearly state how the work in the submitted manuscript differs from the cited work and satisfy reviewers' determination of originality.
- **Experimental** Must be detailed enough to permit other investigators to verify the work, including the source and grade of all chemicals used and detailed descriptions of processes and equipment used to conduct the experiments.
- **Results** The actual data obtained should be given under Results. The interpretation of this data should be under Discussion.
- **Discussion**
  (Results and Discussion may be combined if clarity can be retained).
- **Conclusions** Brief and based on the reported results.
- **Acknowledgement** Necessary credits appear here.
- **References** Required for all citations (matching sequential numbering as used above, but generally limited to no more than about 20 but additional references will be acceptable if critical to the work) adhering to *JALCA* format; Examples:

  1. Liu, C. P., White, R and McClendon, M. D.; Energy Approach to the Characterization of the Thermal Resistance of Leather. *JALCA* **92**(4), 103-118, 2007. [*JALCA* **92**, 103-118, 2007 also acceptable]
  2. Trade Practices for Proper Packer Cattlehide Delivery, 3rd ed., Leather Industries of America and U.S. Hide, Skin & Leather Association, pp. 12-19, 1993.

  This *Journal* is referenced as *JALCA*: for other journals, use the Chemical Abstracts abbreviations. Use of "In press" and web addresses should be limited.

5 -Further Requirements for Manuscripts

Length should generally not exceed 16 single spaced (24 double-spaced) pages of typed text, including embedded Figures &Tables; using 12 point Times New Roman font with paragraphs not indented. The manuscript should contain reproduction quality figures and tables embedded at the appropriate locations in the text, thus offering the entirety of the manuscript as a single Word document.

Figures and Tables (F & T)
Figures (numbered with Arabic numerals) are preferred with images submitted in JPG format as black and white or color. The electronic *JALCA* issue will reproduce color as submitted. Excel table data should preferable be converted to and presented in JPG image format whenever possible.

Tables (numbered with Roman numerals) presented in Excel format should be used only when there is no other way to reasonable present accurate readable data. Excel formatted tables must have a width of no greater than 3.5 inches (9 cm.) or 7.5 inches (19 cm.) and embedded in the Word text in a way that most closely follows the flow of the manuscript. F&T should be numbered consecutively with designated numerals.

To aid the reader, the total number of compliant F&T is recommended to be no more than eight (8) per manuscript unless having additional F&T will help present complex data in a logical fashion. If too many F & T are used, the author(s) will be so advised during the review process.

For a comprehensive overview of all manuscript requirements authors are urged to review manuscripts in recent copies of the *Journal*.

6 - "Life Lines"

Every manuscript should be accompanied by a brief biography of each of the authors or the citation of an earlier "Life Line" biography.

7 - Publication Rights

Authors of papers to be published in the *Journal* will be required to sign a "Transfer of Copyright" form before the paper is published. All papers based on oral presentations at the annual meetings of the ALCA are the property of the Association with the Journal having the exclusive right to publish. Authors employed by a U.S. government agency will be required to provide an employee certification.

Contents of papers published in the *Journal* may not be republished elsewhere without the written permission of the Journal Editor. Permission will be granted for publication of the entire paper in non-English-language publications or for summaries of the paper along with reference to the complete article in *JALCA* in English-language journals.

8 - Peer Review

Two members of the Editorial Board will review editor pre-screened manuscripts. The reviewers' evaluate:

1. Interest to Subscribers (compliance with Subject Matter policy),
2. Originality (Introduction must make this case),
3. Scientific/technical validity (experimental design, results justify conclusions, controls, statistical validity with appropriate use of standard deviations),
4. Literary standards (English language readability, grammar, subject tense/verb matches, etc.),

Reporting the results to the editor on ReviewformXX.

The reviewers' written recommendations will be e-mailed to the corresponding author; who then must respond to all of the reviewers' recommendations with a revised manuscript (response may include separately explanations of specific disagreements with the recommendations). Other than inappropriate subject or lack of originality, most papers can be rendered acceptable for publication by this revision process.

The *Journal* Editor makes the final decisions as to acceptability and scheduling of manuscripts for publication in *JALCA*.

9 – Proofs and Reprints

When formatted, the editor will e-mail a PDF galley proof to the corresponding author. The author will have 3 - 4 days to respond to the editor with suggested final changes. Final changes are restricted to editorial type changes. Technical changes will not be allowed and, if requested, may result in the manuscript being dropped from the planned issue.

Reprints of *Journal* articles may be requested through the ALCA website: **leatherchemists.org** by emailing: **carol.adcock@ttu.edu**

LEATHER

AVELLISYNCO

Selected Dyestuffs

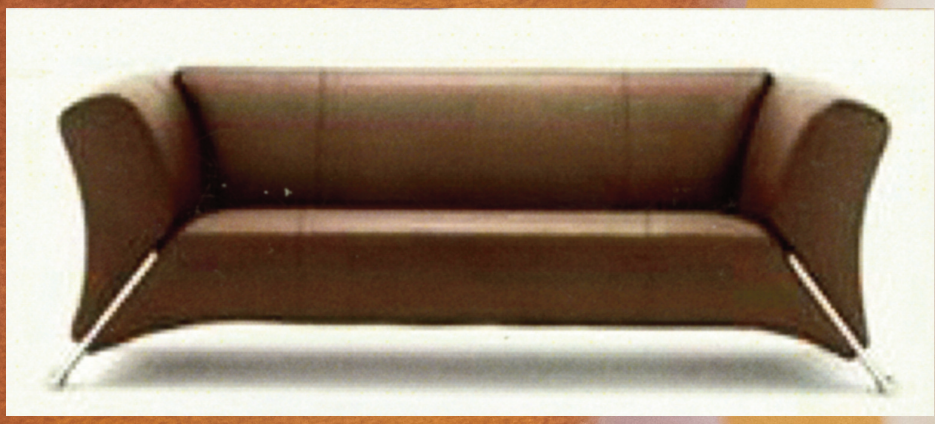

CHEMTAN

17 Noble Farm Drive • Lee, NH 03861 (Office)
57 Hampton Road • Exeter, NH 03833 (Manufacturing)
Tel: (603) 772-3741 • Fax: (603) 772-0796
www.CHEMTAN.com

THE AMERICAN LEATHER CHEMISTS ASSOCIATION
1314 50th Street, Suite 103, Lubbock, Texas 79412-2940
Ph: 806-744-1798 **Fax:** 806-744-1785 **Web:** www.leatherchemists.org
Email: carol.adcock@ttu.edu

Past Issues of *Journal* Needed

If you or someone you know wants to donate past issues of the *Journal* to the Association, please contact us.

Below is a list of issues needed.

Missing Issues:

1906–1909; 1911; 1913; 1915; 1921
1937 – January and December
1939 – January, March and April
1940 – January

Extremely Low Supply:

1931 – February
1936 – January and February
1944 – Jan., Oct., Nov. and Dec.
1945 – June
1946 – January – April
1947 – January, April and August
1948 – January – March
1949 – January – June
1955 – January
1969 – March
1970 – February
1979 – July
1983 – March
1984 – July
1999 – June and July
2000 – January and February
2001 – May and June
2002 – January and March

INDEX TO ADVERTISERS

CALL FOR PAPERS

FOR THE 117th ANNUAL CONVENTION OF THE AMERICAN LEATHER CHEMISTS ASSOCIATION

Grand Geneva Resort & Spa, Lake Geneva, WI
June 20-23, 2023

If you have recently completed or will shortly be completing research studies relevant to hide preservation, hide and leather defects, leather manufacturing technology, new product development, tannery equipment development, leather properties and specifications, tannery environmental management, or other related subjects, you are encouraged to present the results of this research at the next annual convention of the Association to be held at the Grand Geneva Resort & Spa, Lake Geneva, Wisconsin, June 20-23, 2023.

Abstracts are due by April 1, 2023
Full Presentations are due by June 1, 2023

They are to be submitted by e-mail to the
ALCA Vice-President and Chair of the Technical Program:

John Rodden
Union Specialties, Inc.
3 Malcom Hoyt Dr.
Newburyport, MA 01950
E-mail: johnrodden@unionspecialtiesinc.com

The **Abstract** should begin with the title in capital letters, followed by the authors' names. An asterisk should denote the name of the speaker, and contact information should be provided that includes an e-mail address. The abstract should be no longer than 300 English words, and in the Microsoft Word format.

Full Presentations at the convention will be limited to 25 minutes. In accordance with the Association Bylaws, all presentations are considered for publication by *The Journal of the American Leather Chemists Association.* They are not to be published elsewhere, other than in abstract form, without permission of the *Journal* Editor. For further paper preparation guidelines please refer to the *JALCA* Publication Policy on our website: leatherchemists.org

Full Presentations are to be submitted by e-mail to the *JALCA* editor:

Steven D. Lange, *Journal* Editor
The American Leather Chemists Association
E-mail: jalcaeditor@gmail.com
Mobile Phone (814) 414-5689

117th ALCA ANNUAL CONVENTION June 20-23, 2023 Grand Geneve Resort & Spa Lake Geneva, Wisconsin

Featuring the 62nd John Arthur Wilson Memorial Lecture

Retelling "Viewing Leather Through the Eyes of Science"

A Century On

By Mike Redwood, Leather Naturally,
Teacher at University of Bath School of Management,
and Trustee of the U.K. Leather Conservation Centre

Tentative Schedule

Tuesday, June 20
Golf Tournament, Opening Reception and Dinner

Wednesday, June 21
John Arthur Wilson Memorial Lecture
All Day Technical Sessions, Fun Run
Reception and Dinner

Thursday, June 22
All Day Technical Sessions, Annual Business Meeting
Activities Awards Luncheon
Social Hour, Dinner

Visit us at www.leatherchemists.org for full details
under Annual Convention as they become available

CHEMTAN

Weatherproof. Built to Last.

Tel: (603) 772-3741 • www.CHEMTAN.com